Sałacińska, A., Kusiak, M., Whitehouse, M. J., Dunkley, D. J., Wilde, S. A., Kielman, R. (2018): Complexity of the early Archean Uivak Gneiss: Insights from Tigigakyuk Inlet, Saglek Block, Labrador, Canada and possible correlations with south West Greenland. - *Precambrian Research*, *315*, pp. 103—119.

DOI: http://doi.org/10.1016/j.precamres.2018.07.011

Gneiss formation events in the Saglek Block, Labrador; a reappraisal of the Uivak Gneiss

Anna Sałacińska[1], Monika A. Kusiak[1], Martin J. Whitehouse[2], Daniel J. Dunkley[3], Simon A. Wilde[4], Ross Kielman[2], Piotr Król[1]

[1]Institute of Geological Sciences, Polish Academy of Sciences, Twarda 51/55 St., PL-00818 Warsaw, Poland; anna.salacinska@twarda.pan.pl

[2]Swedish Museum of Natural History, SE104 05 Stockholm, Sweden

[3]Faculty of Earth Sciences, University of Silesia in Katowice, PL-41205 Sosnowiec, Poland

[4]School of Earth and Planetary Sciences, Curtin University, PO Box U1987, WA 6845, Perth, Australia

Keywords: Saglek Block, U-Pb geochronology, Uivak Gneiss, TTG gneiss

Abstract

The Saglek Block of Labrador is an Archean gneiss complex, metamorphosed during a *ca.* 2.7 Ga event. The main component of the complex is the Eoarchean Uivak orthogneiss, which includes lenses of the Nulliak supracrustal assemblage. Both lithologies are cut by the mafic Saglek metadykes. The Uivak gneisses have been divided into Uivak I grey gneiss and Uivak II augen gneiss. The former underwent *ca.* 3.6 Ga high-T metamorphism prior to the intrusion of the latter. However, the exact age, nature and extent of Uivak II gneiss is poorly understood. We present geochemical and geochronological results for both orthogneisses. These data help refine various hypotheses concerning the formation of Eo- to Paleoarchean protoliths. Magmatic ages of 3746±5 and 3717±6 Ma are consistent with previous estimates for the age of Uivak I gneiss. Uivak II augen gneiss from Maidmonts Island, where there is a clear intrusive relationship between the Uivak II and Uivak I gneissic protoliths, has an age of 3325±3 Ma. This age is equivalent to that of a homogeneous grey gneiss from St John's Harbour, with an age of 3318±5 Ma. Grey gneiss from Big Island ~~has a~~ distinctively younger ~~age of~~ 3219±7 Ma, equivalent to the *ca.* 3.24 Ga Lister Gneiss. Our study shows that granitic gneisses classified as Uivak II were emplaced 200-300 ~~Myr~~ after *ca.* 3.6 Ga metamorphism and deformation ~~in~~ the Uivak

I gneiss. The igneous protolith of Uivak II gneiss predates the Lister Gneiss by about 100 Myr. The Uivak I and Lister gneisses are geochemically similar, and are both TTGs, whereas the Uivak II gneiss is a granitoid partially derived from pre-existing crust. We propose abandoning the term ‘Uivak II gneiss’, and renaming ca. 3.3 Ga granitoids, after the type-locality, as Maidmonts Gneiss. This restricts the term ‘Uivak Gneiss’ to TTG Eoarchean gneisses.

1. Introduction

The Archean Nain Province is located along the eastern coast of Labador (Canada), and forms the western margin of the North Atlantic Craton. The province is correlated with Archean terranes in southern West Greenland (Bridgwater et al. 1973; Nutman et al. 2004a; Hölttä et al. 2008) across the Labrador Sea. To the west and south, the Nain Province is bordered by early- to mid-Proterozoic orogenic belts named the Churchill, Grenville and Makkovik provinces (Taylor 1971; Greene 1974). The Nain Province is divided into two Archean blocks, the northern Saglek Block and the southern Hopedale Block (Fig. 1), which are separated by the middle-Proterozoic Nain Plutonic Suite (Bridgwater and Schiøtte 1991; Wasteneys et al. 1996). The Saglek Block comprises dominant early Archean Uivak TTG gneisses, with subordinate belts of mafic and metasedimentary supracrustal rocks that include the so-called ‘Nulliak assemblage’. Comparable lithologies are found across the Davis Strait in South West Greenland, where the early Archean Itsaq Gneiss Complex (IGC) (Nutman et al. 1996) comprises Amîtsoq TTG gneisses (McGregor 1973) associated with the metasupracrustal Akilia association (McGregor and Mason 1977), which includes the Isua Greenstone Belt (Fedo et al. 2001). The Itsaq Gneiss Complex contains the most extensive and well-studied early Archaean rock record (Nutman et al. 1996,2004a), including some of the oldest identified rocks on Earth. The area comprises several generations of granitoid intrusions, emplaced between *ca.* 3.9 Ga and 3.5 Ga (e.g., Nutman et al. 1996, 2000, 2004a, 2007, 2013; Whitehouse et al. 1999; Crowley 2003; Whitehouse and Kamber 2005; Næraa et al. 2012), which formed the protoliths of a major part of the Itsaq Gneiss Complex, together with younger orthogneisses and migmatites that were emplacement between *ca.* 3.2 Ga and 2.8 Ga (Polat et al. 2010; Næraa et al. 2012). Most of these rocks acquired their structural elements and fabrics during Neoarchean tectonothermal events (around 2.8-2.7 Ga) (McGregor 1973; Chadwick and Nutman

1979; Whitehouse and Kamber 2005) with local low-strain domains that preserve evidence of *ca.* 3.6 Ga high-T metamorphism (e.g., Griffin et al. 1980; Nutman et al. 1996, 2002, 2013; Crowley 2003; Friend and Nutman 2005; Whitehouse and Kamber 2005).

In contrast, the Saglek Block in Labrador has not been so extensively studied. Early mapping (Bridgwater et al. 1975; Hurst et al. 1975; Bridgwater and Collerson 1976, 1977) followed by geochronological studies (Collerson and Bridgwater 1979; Shiotte et al. 1989a,b; Bridgwater and Schiøtte 1991) defined and dated major lithologies. More recently, a resurgence of interest in the Saglek Block has led to several detailed studies (Krogh and Kamo 2006; Shimojo et al. 2016; Komiya et al. 2017; Kusiak et al. 2018; Sałacińska et al. 2018) that revised earlier interpretations and produced new controversies, especially regarding the oldest components of the block. Following the study of Sałacińska et al. (2018) that advanced understanding of the age and composition of the Uivak I gneiss, this study focuses on orthogneisses previously identified as the younger, but poorly understood, Uivak II gneiss. We present geochemical and geochronological results that test various hypotheses concerning the formation of early to mid-Archean gneissic protoliths. We provide improved geochronological and geochemical characterisation of rocks formerly assigned to the Uivak II gneiss, and suggest a new definition for the gneisses that were produced much later than the predominant Uivak I gneiss.

2. Geological setting

The Saglek Block is located in the northern part of the Archean Nain Province, exposed along the coast northwards from the Nain Plutonic Suite, between Okak Island and Nachvak Fjord (Fig. 1; Bridgwater and Schiøtte 1991; Wasteneys et al. 1996). The block is divided at Saglek Bay into two segments by the major N-S trending Handy Fault, which separates rocks of different crustal levels. The western part of the Saglek Block consists of granulite-facies rocks, whereas the eastern part reveals a transition from amphibolite-facies in the north (from Big Island through Tigigakyuk Inlet to Lister Island) to granulite-facies southward to Hebron Fjord (Bridgwater et al. 1975; Schiøtte et al. 1989a). The Saglek Block contains a strongly deformed Archean gneiss complex, consisting predominantly of quartzofeldspathic gneisses of presumed igneous origin, which are tectonically juxtaposed and interleaved with supracrustal rocks. The major component of the complex is the early Archean Uivak orthogneiss, which has been subdivided into the older Uivak I TTG gneisses and younger Uivak II gneisses. Macro-scale tectonic lenses of the Nulliak supracrustal assemblage are intercalated with the Uivak gneisses, and both cut by metamorphosed plagioclase-phyric mafic Saglek dykes (Bridgwater et al. 1975; Bridgwater and Collerson 1976, 1977). These units have been correlated with the Itsaq Gneiss Complex in southern West Greenland (Sałacińska et al. 2018 and references therein), which is intruded by the plagioclase-phyric Ameralik dyke swarm (Nutman et al. 2004b), a likely Saglek dyke correlative. The oldest recognized post-Saglek dyke orthogneiss from the Saglek Block is the Paleoarchean felsic Lister Gneiss (Schiøtte et al. 1989a). Contacts between the older Uivak and younger Lister gneisses are tectonic, and no evidence for intrusive relationships has been recognized (Bridgwater and Schiøtte 1991). The Upernavik supracrustal assemblage is a composite group of rocks of several ages, which is more extensively exposed than the older Nulliak assemblage. The Upernavik supracrustal assemblage is dominated by pelitic and psammitic units. The original distinction between the older Nulliak and younger Upernavik assemblages was based on the absence of Saglek dykes within the younger rocks (Bridgwater et al. 1975; Bridgwater and Collerson 1976, 1977; Schiøtte et al. 1989a,b). Further investigation showed that some "Upernavik-like" lithologies are cut by a mafic dykes assigned to the Saglek swarm (Bridgwater and Schiøtte 1991). Therefore, lithological differences, such as the presence of banded ironstones and metacherts in the Nulliak assemblage, are more appropriate in separating these two units (Bridgwater and Collerson 1976, 1977; Ryan and Martineau 2012). The present outcrop pattern is a result of tectonic intercalation and subsequent folding of orthogneisses and supracrustal rocks during a late Archean metamorphic event at *ca.* 2.8-2.7 Ga and/or *ca.* 2.5 Ga reaching granulite-facies conditions (Krogh and Kamo 2006; Connelly and Ryan 1996; Bridgwater and Schiøtte 1991; Schiøtte et al. 1989a,b).

3. Definition and characteristics of 'Uivak Gneiss'

The original definition of the Uivak Gneiss in the Saglek Block was given by Bridgwater et al. (1975): "The Uivak gneisses are a composite group of quartzofeldspathic rocks which may not all belong to the same igneous suite. They are described as a single lithological unit because of their relation with [intrusion by] the Saglek dykes". The Uivak gneisses consist of felsic grey gneisses (Uivak I Gneiss), along with porphyritic granitoid gneisses, and calc-alkaline intrusions (Uivak II Gneiss; Bridgwater and Collerson 1976). The Uivak I gneisses are grey, compositionally varied, fine- to medium-grained, quartzofeldspathic and partially migmatized. Homogenous parts of the gneiss are dominated by TTG compositions. More mafic phases, including gabbroic, dioritic and monzonitic gneisses, are locally present. Field observations in areas of relatively low finite strain show that the Uivak I Gneiss was affected by at least one major period of deformation and migmatisation prior to the intrusion of the Uivak II gneissic protolith (Bridgwater et al. 1975; Bridgwater and Collerson 1976; Collerson and Bridgwater 1979).

The less extensive Uivak II Gneiss occurs in a relatively narrow, localised belt, parallel to gneissosity, extending SSE from the southern coast of Big Island, through White Point, Mentzel Island, and Maidmonts Island to the coast opposite Nulliak Island (Fig. 1). Originally, the Uivak II Gneiss was defined as a co-genetic suite of plutonic bodies that include iron-rich porphyritic granodiorites and ferro-diorites intruded into deformed and migmatised Uivak I Gneiss, although any original intrusive relationships were largely obscured by strong deformation (Bridgwater et al. 1975; Hurst et al. 1975; Bridgwater and Collerson 1976; Collerson and Bridgwater 1979). The four main components of the Uivak II Gneiss were identified as: a) coarse-grained granitic gneiss with large feldspar augen; b) hornblende-rich ferrodiorites; c) feldspar-phyric biotite-rich inhomogenous quartz monzonite sheets; and d) thin hornblende-rich dykes (Bridgwater et al. 1975; Bridgwater and Collerson 1976). The last three types were identified from the southern part of Big Island. A Rb-Sr whole-rock errorchron of *ca.* 3622 Ma, derived from a combination of Uivak I and II samples led Bridgwater and Collerson (1976) to suggest that both types were broadly contemporaneous. However, further detailed geochronology (Baadsgaard et al. 1979) showed that the iron-rich suite from Big Island is a comparatively late (*ca.* 2.8-2.5 Ga) minor association, and was therefore excluded from the Uivak II gneiss. Subsequently, the assumption that Uivak II protoliths formed at *ca.* 3.6 Ga has never been tested.

The first evidence of an early Archean age for the Uivak I Gneiss was provided by whole rock Rb-Sr isotopic dating (3545±72 Ma; Hurst et al. 1975; and 3533+315/-238 Ma; Collerson et al. 1982) and this was confirmed by multigrain U-Pb zircon dating using Isotopic Dilution Thermo-Ionisation Mass Spectrometry (ID-TIMS) (>3485 Ma; Baadsgaard et al. 1979). The first precise age of the formation of Uivak I Gneiss (3732±6 Ma) was determined by Schiøtte et al. (1989a). Further high-precision ages were ~~provided by Secondary Ion Mass Spectrometry (SIMS;~~ Kusiak et al. 2018 and Sałacińska et al. 2018). Isotopic U-Pb dating of zircon grains also identified a significant amount of older zircon, up to *ca.* 3.92 Ga in age (Collerson 1983; Schiøtte et al. 1989a; Shimojo et al. 2016); however such ages may be largely xenocrystic. A re-interpretation of the age of the Uivak I Gneiss was presented by Krogh and Kamo (2006), who, on the basis of new zircon dating of grey gneisses in Saglek Bay, suggested that they represent two unrelated generations of magmatism, the first at 3634±31 Ma (with inheritance back to 3730 Ma), and the second at 3348±7 Ma, on the west and east sides of the Handy Fault, respectively. Further re-investigation of grey gneisses mapped as Uivak Gneiss by Laser Ablation Inductively Coupled Plasma Mass Spectrometry (LA-ICPMS) U-Pb dating of zircon was conducted by Komiya et al. (2017). Their results led them to propose a new model of 'prolonged' granitoid formation with gneisses grouped into five (Uivak A-E) age ranges of approximately 50 my each over a 300 million year period between 3.9 – 3.6 Ga. Previous attempts at U-Pb zircon dating of Uivak II gneiss have not provided clear results. Wanless et al. (1979) calculated an upper intercept age of 3760±150 Ma, whereas a few discordant zircon analyses by Collerson (1983) recorded $^{207}Pb/^{206}Pb$ ages of *ca.* 3350 Ma.

The Lister gneiss, identified as a subvertical sheet of felsic orthogneisses amongst amphibolite facies gneisses, is significantly younger (*ca.* 3.24 Ga) than Uivak I gneiss and post-dates the Saglek dykes (Schiøtte et al. 1989a). The type locality on Lister Island (Schiøtte et al. 1989a) yielded an age for the gneiss of 3235±8 Ma, with other localities yielding slightly younger ages (3219±3 Ma and 3213±4 Ma; Schiøtte et al. 1990; Wasteneys et al. 1996, respectively). Similar felsic gneisses, also *ca.* 3.2 Ga in age, were subsequently identified from the south side of Saglek Bay (Bridgwater and Schiøtte 1991), on Big Island (Krogh and Kamo, 2006), on Nulliak Island (Komiya et al., 2017), on granulite-facies Parkavik Island (Schiøtte et al. 1990) and offshore of the Saglek Block (drill core; Wasteneys et al. 1996), which indicated that *ca.* 3.24 Ga gneisses are volumetrically more widespread than previously thought.

4. Sample locations

Sampling was conducted between Saglek Bay and Hebron Fjord (Fig. 1). Rock types were chosen that were representative of both grey gneisses (typical of Uivak I) and augen gneisses (typical of Uivak II). A total of six samples were collected for this study: from St John's Harbour (L1410, L1411), Big Island (L1443, L1444), Little Island (L1463) and Maidmonts Island (L1467) (Fig. 1). Samples from St John's Harbour represent homogenous fine-grained gneiss (L1410) and banded grey gneiss (L1411). From field observations, the latter sample (L1411) may have more than one igneous protolith juxtaposed during a later deformation event. The samples from Big Island represent weakly pophyroblastic (L1443) and homogenous (L1444) fine-grained grey gneisses and were collected from the coast between localities previously sampled by Komiya et al. (2015, 2017), who obtained *ca.* 3.22 Ga and *ca.* 3.73 Ga ages. An intrusive relationship between these two grey gneisses was not identified and none of the sampled outcrops are cut by mafic dykes or pegmatite (Fig. 2C,D). On Little Island, one homogenous fine-grained grey gneiss (L1463) was sampled from an outcrop containing grey gneiss with fragments of mafic dykes and pegmatite (Fig. 2E). A similar outcrop was found by Krogh and Kamo (2006), who determined the age of orthogneiss at *ca.* 3.35 Ga, cut by a mafic dyke at *ca.* 2.70 Ga and by pegmatite at *ca.* 2.56 Ga. However, orthogneiss (L1463) from our sample locality is different from the orthogneiss dated by Krogh and Kamo (2006), because it is interleaved with coarser-grained pegmatite veins 1-2 cm wide. Porphyroclastic gneiss (L1467; Fig. 2F) was collected from Maidmonts Island, where the largest body of Uivak II Gneiss occurs, and it extends at least 3 km along strike (Fig. 3; Bridgwater and Collerson 1976). At this locality, a deformed and transposed contact between augen gneiss (L1467), grey gneiss and syn-tectonic white granitoid, was identified (Fig. 2F). In another outcrop on the island, we noted a clear intrusive relationship between the younger Uivak II and Uivak I gneisses (Fig. 3).

All six samples, including homogenous (L1410, L1444 and L1463), weakly porphyroblastic (L1443), and banded (L1411) fine-grained grey gneisses and porphyroclastic gneiss (L1467), have granoblastic textures. Sample locations, rock types as classified by bulk-rock geochemistry, and mineral assemblages are listed in Table 1.

5. Analytical procedures

For geochemical analyses, the most uniform parts of the samples were selected and all weathered material was removed. They were then crushed and milled in an agate ball mill. The material was then coned and quartered before being despatched for analysis of major and trace elements at the Bureau Veritas Analytical Laboratories in Vancouver, Canada. X-ray fluorescence (XRF) spectrometry was used for major elements whereas inductively coupled plasma mass spectrometry (ICP-MS) was used for trace elements, including REE. The volatile content of each sample was determined by loss on ignition (LOI). The data were then plotted in diagrams using the GeoChemical Data toolkit (GCDkit) (Janoušek et al. 2016).

Separation of zircon was conducted at the Sample Separation Laboratory, Institute of Geological Sciences PAS (Krakow). Crushed material was run through Carpco and Frantz magnetic separators to remove magnetic minerals. To isolate dense minerals, TBE (tetrabromoethane) was used. Zircon was then separated from other heavy minerals by hand-picking under a binocular microscope. The zircons were then placed together with the reference material (zircon 91500, Wiedenbeck et al. 1995) in epoxy resin mounts and then were polished to expose the cores of the zircons. All zircon grains were imaged and documented in transmitted and reflected light and by scanning electron microscopy. For scanning electron microscopy, the grains were carbon coated prior to being imaged using cathodoluminescence (CL) to highlight the internal structure of the crystals. Before analyses, the epoxy mounts were cleaned in an ultrasonic bath and gold coated for U-Th-Pb isotopic analysis.

U-Th-Pb isotopic analysis of zircon was undertaken at the Department of Geosciences in the Swedish Natural History Museum (Stockholm, Sweden), using a CAMECA IMS 1280 secondary ion mass spectrometer (SIMS) in the NordSIM analytical facility. The analytical method is according to Whitehouse and Kamber (2005). The analytical conditions during analysis consisted of using a nominal ~20 µm, 6 nA O_2- ion beam in dynamic mono-collection mode and an ion counting electron multiplier (EM) ion counter at a mass resolution of ~5400 (M/ΔM). The protocol of Jeon and Whitehouse (2015) was used for calibrating the Pb/U ratios using the Pb/UO vs. UO_2/UO method based on zircon standard 91500. The 91500 zircon has a U concentration of 80 ppm and an age of 1065 Ma (Wiedenbeck et al. 1995). Common Pb was corrected using the ^{204}Pb counts where these exceeded 3x the standard deviation on the average background. Common Pb composition assumes the present-day terrestrial Pb-isotope composition model (Stacey and Kramers 1975), following the rationale of Zeck and Whitehouse (1999) that this is largely surface contamination introduced during sample preparation and not common Pb residing in zircon and/or micro-inclusions. During spot analyses, very low concentrations of common Pb (f^{206}Pb <0.1%) were detected and have little influence on the ages. The in-house software developed by M.J. Whitehouse was used for data reduction, and the ages were calculated using Isoplot (Ludwig, 2012). In the tables, the data are quoted with 1σ analytical errors, whereas weighted mean calculations and discordia intercept ages are quoted at 95% (2σ) confidence levels, and include the decay constant error. Data with common Pb content >1%Pb were excluded from ^{207}Pb/^{206}Pb pooled age calculation, as were data with absolute discordance >5%.

6. Results

6.1. Whole-rock Geochemistry

Whole-rock major and trace element compositions for gneisses from Saglek Bay are given in Table 2.

All samples are silica-rich (66.0-73.7 wt. % SiO_2) and have variable contents of aluminium (13.5-18.5 wt. % Al_2O_3). The variable contents of sodium (3.6-5.7 wt. % Na_2O) and potassium (1.4-4.1 wt. % Na_2O) are reflected in the range of K_2O/Na_2O ratios (0.25-1.09), with the highest ratios in samples L1410 and L1467. The gneisses also have variable contents of ferromagnesian oxides, ranging from 1.9 to 5.4 wt.% (Fe_2O_3*+MgO+MnO+TiO_2 wt.%, Fe_2O_3* = total Fe expressed as Fe_2O_3).

Samples plot in the granodiorite (L1443 and L1444) and granite (L1410, L1411, L1463 and L1467) fields in the TAS diagram (Middlemost 1994) and are close to the boundaries between granite, granodiorite and quartz monzonite (Fig. 4A). All samples are weakly peraluminous (Fig. 4B). In the AFM diagram (Irvine and Baragar 1971), the samples follow the calc-alkaline trend (Fig. 4C), although two of them (L1410 and L1467) are located closer to the A-F side of the ternary diagram. In the normative An-Ab-Or ternary diagram (Barker 1979; after O'Connor 1965), the samples plot in the trondhjemite (L1443, L1444 and L1463) and granite (L1410, L1411 and L1467) fields. This diagram is used for classification of our samples following Jahn et al's. (1981) classification of Archean TTG gneisses. Samples L1463 and L1411 are close to the trondhjemite-granite boundary (Fig. 4D).

The trace elements were normalized to the primitive mantle (PM) values from McDonough and Sun (1995) (Fig. 5A). Four samples (L1411, L1443, L1444, L1463) have similar trace element profiles, with strongly negative Nb-Ta and P anomalies, weak to moderate negative Ti anomalies and a minor peak in Sr. Sample L1410 is geochemically similar to sample L1467, with low U, Nb, Ta, Sr, P, and weak negative Ti anomalies. These two samples have the highest contents of Th and Zr. All samples are strongly enriched in Rb (94-174 ppm) and Ba (196-1232 ppm) relative to PM (Table 2).

The rare earth elements (REEs) were normalized to the chondrite values from McDonough and Sun (1995). The gneisses have relatively high light rare earth element contents (LREE) (11.0-99.1 ppm La) and low heavy rare earth element (HREE) contents (0.22-0.39 ppm Yb), with La/Yb ratios ranging from 28 to 310 (Table 2, Fig. 5B). Two samples, L1410 and L1467, show the strongest fractionation of L/HREE (La/Yb ratios of 309.7 and 144.9, respectively) and have distinct negative Eu anomalies, whereas the other four samples do not.

6.2. U-Pb geochronology

The sample results are presented in order of sample collection. SIMS U-Th-Pb isotopic data are given in Tables 3 - 8 for samples L1410, L1411, L1443, L1444, L1463 and L1467, respectively.

Granitic gneiss sample L1410 from St John's Harbour contains mostly subhedral to anhedral elongate zircons (up to 230 μm in length, with a typical aspect ratio of 2:1). Most grains are zoned, with uniform to weakly-zoned dark CL cores (Fig. 6A, grain 3, 8), whereas other grains have relatively bright CL cores that grade into dark CL rims (Fig. 6A, grain 4). Twenty-four analyses were undertaken on 21 grains from dark and bright CL cores and gradational zones, yielding 17 concordant data (Table 3; Fig. 7A) and 7 data that were either discordant and/or have high common Pb. The 17 concordant analyses have relatively low U contents (30-140 ppm), with the exception of a grain 03c (622 ppm), and have Th/U values ranging from 0.43 to 0.97. Fourteen concordant data scatter along the concordia with $^{207}Pb/^{206}Pb$ ages from 3336 to 3260 Ma. Three data are significantly younger, with $^{207}Pb/^{206}Pb$ ages in the range 3064-3004 Ma. No correlation between zircon structure and age was observed (Fig. 6A). From 14 concordant analyses, the 7 oldest data are statistically equivalent with a weighted mean $^{207}Pb/^{206}Pb$ age of 3318±5 Ma (MSWD=1.7). Of the 7 remaining data from this group, and the 3 youngest concordant ones, there is no distinction in composition or structure between these and the older data. Assuming that the older data represent the time of zircon crystallization, the younger data may have been affected by Pb loss during a major metamorphic event at *ca.* 2.7 Ga (Schiøtte et al. 1989a; Krogh and Kamo 2006). These data scatter along a Model 2 discordia chord with intercept ages of 2725±160 & 3392±65 Ma (MSWD = 1.8). The upper intercept age is slightly older than the weighted mean $^{207}Pb/^{206}Pb$ age; however, the latter is preferred as the best estimate for the emplacement of the granitic protolith of the gneiss.

Granitic gneiss sample L1411 from St John's Harbour contains mostly subhedral elongate zircon grains (up to 300 μm long, with aspect ratios of 2:1 to 4:1; Fig. 6B). Most are dark in CL, although a few have lighter cores. Thirty-six analyses of 31 grains were obtained (Table 4; Fig. 7B), of which 5 analyses were discordant and 15 have high common Pb. The remaining 16 analyses were obtained from zones with Th/U values ranging from 0.16 to 0.75, and spread along the concordia with $^{207}Pb/^{206}Pb$ ages between 3789 Ma and 3602 Ma. The oldest age is from a structurally distinct core with low U (50 ppm) (Fig. 6B, grain 21). Three data are from cores with similar U contents (148-180 ppm) and have $^{207}Pb/^{206}Pb$ ages of 3753-3746 Ma. The remaining 12 concordant analyses are from weak, non-oscillatory zoned zircon, with highly variable U contents between 233 to 1076 ppm. These have $^{207}Pb/^{206}Pb$ ages which spread along the concordia from 3728 to 3602 Ma.

Trondhjemitic gneiss sample L1443 from Big Island contains zircons that are subhedral and elongate (100-230 μm length, with aspect ratios of 2:1 to 3:1; Fig. 6C), and strong oscillatory zoning. A total of 32 analyses were obtained from 20 grains (Table 5; Fig. 7C), of which 5 concordant data are excluded from further consideration because they were obtained from mixed domains. Of the remaining data, 10 are discordant and 17 have high common Pb. Ten concordant data from 7 zircon grains spread along the concordia with $^{207}Pb/^{206}Pb$ ages ranging from 3759 to 3730 Ma. These zircon grains have variable U concentrations (126-422 ppm) and Th/U ratios (0.09-0.67). The 6 oldest are statistically equivalent, with a weighted mean $^{207}Pb/^{206}Pb$ age of 3746±5 Ma (MSWD=1.5), whereas the remaining 4 concordant data range to younger ages, which are interpreted as being affected by Pb loss.

Trondhjemitic gneiss sample L1444 from Big Island contains mostly subhedral, elongate zircons (up to 250 μm with an average aspect ratio of 2:1) with strong oscillatory zoning. They have thin rims which transgress the primary structures (Fig.6D). Nineteen analyses from 10 grains were obtained (Tab.6; Fig.7D), including 9 concordant data and 10 data with high common Pb contents. The zircon grains have variable U contents (78-508 ppm) and Th/U ratios ranging from 0.38 to 0.55. Two concordant analyses with $^{207}Pb/^{206}Pb$ ages of 3174 Ma and 3160 Ma were obtained from mixed zones and over cracks, and were therefore excluded from further consideration. The remaining seven concordant data define a weighted mean $^{207}Pb/^{206}Pb$ age of 3219±7 Ma (MSWD=1.4).

Trondhjemitic gneiss sample L1463 from Little Island contains zircons that are mostly subhedral and elongate (up to 250 μm in length and with an average aspect ratio of 2:1 to 3:1; Fig. 6E), and show oscillatory zoning in CL. Most grains have a thick, dark-CL rim and areas of disrupted oscillatory zoning. Thirty-eight analyses were made on 23 grains, of which 5 were identified as mixed zones in post-analytical CL imaging, and are therefore excluded from further consideration. Nineteen of the remaining analyses are either discordant or have high common Pb. Fourteen analyses are concordant (Tab.7; Fig.7E) and spread along the concordia with $^{207}Pb/^{206}Pb$ ages ranging from 3749 Ma to 3517 Ma. Of these data, 2 analyses were obtained from a same bright-CL core with low U contents (44 and 22 ppm, respectively) and yield $^{207}Pb/^{206}Pb$ ages of 3749 Ma and 3675 Ma (Fig. 7E). Five analyses from oscillatory zoned cores, with $^{207}Pb/^{206}Pb$ ages ranging from 3725 Ma to 3713 Ma form a significant cluster on concordia, with a weighted mean $^{207}Pb/^{206}Pb$ age of 3717±6 Ma (MSWD=2.4). Four concordant data (3703 Ma, 3696 Ma, 3691 Ma and 3517 Ma) are on areas of prismatic zircon in the cores of grains with morphologies and compositions similar to those which form the cluster at *ca.* 3717 Ma. Additionally, three analyses from dark-CL rims (Fig. 7E), with high U contents (936-1046 ppm) have $^{207}Pb/^{206}Pb$ ages ranging from 3634 Ma to 3562 Ma.

Granitic gneiss sample L1467 from Maidmonts Island mostly contains subhedral, elongate zircon grains (up to 380 μm in length, with an aspect ratio of 2:1 to 3:1; Fig.

6F). Some zircon grains have unzoned, dark-CL cores with distinct boundaries and surrounded by oscillatory zoned or unzoned zircon or else they are zoned with relatively bright CL cores showing a gradation to dark CL rims (Fig.6F). Twenty-eight analyses from 27 grains were obtained (Table 8; Fig. 7F), of which 11 are discordant or have high common Pb. Seventeen concordant data spread along concordia with $^{207}Pb/^{206}Pb$ ages ranging from 3328 Ma to 3256 Ma. These zircons have a range of U contents between 36 ppm and 1250 ppm, and Th/U ratios from 0.58 to 0.97. Of these, the 10 oldest concordant analyses yield a weighted mean $^{207}Pb/^{206}Pb$ age of 3325±3 Ma (MSWD=1.4). The remaining seven concordant analyses have similar structure to the *ca.* 3325 Ma zircon but slightly younger ages, which are interpreted as being affected by Pb loss during later metamorphism at ca. 2.7 Ga.

7. Interpretation

7.1. Geochemistry

The grey gneisses in the Saglek Block are extensively recrystallised and deformed as a result of several later events, including upper amphibolite to granulite facies regional metamorphism (Collerson and Bridgwater 1979; Schiøtte et al. 1989a). Consequently, the primary magmatic composition of rocks may have been altered. Metamorphism and hydrothermal alteration can affect large ion lithophile elements (LILE), including Rb, Ba, K, Sr, Pb and Th, as well as light rare earth elements (LREE). In contrast, high field strength elements (HFSE) and heavy rare earth elements (HREE) are relatively immobile (Alderton et al. 1980; Ward et al. 1992; Condie and Sinha 1996; Polat and Hofmann 2003). However, on the REE chondrite-normalized trace element diagrams, the LREE display only limited variation between samples, suggesting these elements were relatively immobile on the whole rock scale.

The whole rock geochemistry, including major and trace element compositions, distinguishes two types of gneiss: TTG gneiss (L1411, L1443, L1444, L1463) and granitic gneiss (L1410, L1467). TTG gneisses vary from trondhjemitic to borderline granitic (Fig. 4D). These have strongly fractionated REE patterns without Eu anomalies, and have negative Nb, Ta, P and Ti anomalies. All of these features are typical of Archean TTG, although L1411 has a higher K_2O content. In contrast, the granitic gneisses L1410 and L1467 are characterized by higher Na_2O/K_2O ratios, extreme enrichment in LREE, high La/Yb ratios and negative Eu anomalies.

Experimental studies on partial melting of hydrous metabasalt as a source for TTG show that HFSEs are largely controlled by mineral assemblages in the restite. The fractionated REE pattern requires the presence of garnet in the source (Martin 1987; Drummond and Defant 1990; Rapp et al. 1991; Moyen and Stevens 2006) for which both garnet amphibolite (Foley et al. 2002) and eclogite residues (Rapp et al. 2003) provide reasonable solutions. The negative Nb, Ta and Ti anomalies have been attributed by Martin et al. (2005) and Hoffman et al. (2011) to the presence of residual amphibole and/or Fe-Ti oxides (rutile, ilmenite).

The lack of significant Eu anomalies in the four TTG samples (L1411, L1443, L1444, L1463) indicates that plagioclase was not stable in the residue. In contrast, samples L1410 and L1467 (granitic gneisses) have significant negative Eu anomalies, which indicate that there has been some role for plagioclase, either residual after partial melting and/or *via* fractional crystallization.

According to the Moyen (2011) classification, the TTG gneisses from Saglek Block belong to the medium-pressure (L1411, L1443) and high-pressure (L1444 and L1463) subgroups; both are TTG gneisses *sensu stricto*. Partial melting of mafic crust with residual amphibole and garnet, and little or no rutile or plagioclase, can produce the medium-pressure type of TTG. The high-pressure subgroup can be produced by the melting of mafic crust leaving residual garnet and rutile, with no amphibole or plagioclase. In contrast, the granitic gneisses (L1410 and L1467) with Eu anomalies, can be classified as high LREE, being transitional sodic (low-pressure) to potassic (higher LILE) types. The latter can be produced by partial melting within continental crust. This suggests that an earlier crustal component played an important role in formation of these two samples.

7.2. Geochronology

The oldest age population from the samples studied was found in trondhjemitic gneiss L1443 from Big Island (Fig. 6C) which yielded a magmatic age of 3746±5 Ma from oscillatory zoned zircon typical of that crystallized from a felsic magma.

Consequently, this age is interpreted as the crystallization age of the trondhjemitic orthogneiss protolith, with older analyses deriving from xenocrystic cores.

Sample L1463 from Little Island shows a more complex age distribution, with a range of $^{207}Pb/^{206}Pb$ ages from 3749 to ~~3675~~ Ma, and a subpopulation of 5 oscillatory zoned, magmatic, cores that yielded a mean age of 3717±6 Ma that we interpret as the time of protolith crystallization. Older cores are interpreted as xenocrystic zircon, whereas younger cores are interpreted as subsequent Pb loss. High U rims, typical of metamorphic zircon scatter around *ca.* 3.6 Ga and provide evidence of metamorphism and isotopic disturbance at this time. This corresponds to previous estimates for the timing of high-T metamorphism in the area (Schiøtte et al. 1989a, Sałacińska et al. 2018).

In the case of granitic gneiss sample L1411 from St John's Harbour no clear age for the igneous protolith was obtained. However, weakly zoned zircon ages scattered between 3753 Ma to 3602 Ma, if magmatic, suggest an age greater than *ca.* 3.6 Ga. The older, distinct high CL core yielded a xenocristic age of *ca.* 3750 Ma.

The trondhjemitic gneiss sample L1444 from Big Island contains zircon with oscillatory zonation (Fig. 6D) typical of igneous growth, therefore the weighted mean age of 3219±7 Ma, is interpreted as the age of the magmatic protolith. This age is significantly younger than other TTG gneisses, and corresponds to that of the Lister Gneiss (Schiøtte et al. 1989a).

Granitic gneiss sample L1410 from St John's Harbour contains zircon with CL-dark weakly zoned cores and distinct bright rims (Fig. 6A). The oldest wieghted mean $^{207}Pb/^{206}Pb$ age of 3318±5 Ma, interpreted as the crystallization age of the magmatic protolith, with scattered younger ages attributed to metamorphism at *ca.* 2725 Ma. Similarly, the oldest population of zircon from granitic gneiss L1467 from Maidmonts Island, which ~~include~~ oscillatory zoned and unzoned cores (Fig. 6F), yields a weighted mean $^{207}Pb/^{206}Pb$ age of 3325±3 Ma, which is interpreted as the time of granite emplacement.

These results show that the orthogneisses can be separated into two groups: an older set with Eoarchean magmatic ages and indication of metamorphism at *ca.* 3.6 Ga; and two younger samples of granitic gneiss with ages of *ca.* 3.3 Ga. The former are all grey orthogneisses and fit with published ages and descriptions of Uivak I gneiss (Kusiak et al. 2018; Sałacińska et al. 2018 and references therein). The two younger samples are of homogeneous grey gneiss (L1410) and porphyroblastic augen gneiss (L1467), but their geochemistry and zircon structures are similar and the equivalent ages (3318±5 Ma and 3325±3 Ma, respectively) suggest that they were co-genetic. Taking into account intrusive relationships between porphyroblastic gneiss and grey gneiss observed in Maidmonts Island (Fig. 3), these younger samples are interpreted as Uivak II gneiss.

8. Discussion

The Eoarchean (>*ca.* 3.6 Ga) Uivak Gneiss consists of a diverse group ranging from fine-grained to weakly porphyroblastic, homogenous to banded and of felsic composition. Igneous protoliths underwent metamorphism up to granulite facies, resulting in their gneissosity. From initial field observations (Bridgwater et al. 1975; Bridgwater and Collerson 1976; Collerson and Bridgwater 1979), as well as the detailed examination of zircons with complex core/mantle/rim structures (e.g. Schiøtte et al. 1989a, Sałacińska et al. 2018, and in this study), a high-T metamorphic event at *ca.* 3.6 Ga was identified. This tectonothermal event pre-dates emplacement of the Uivak II gneiss. This is confirmed by our field observations on Maidmonts Island (Fig. 3), which show porphyritic granite (the precursor to Uivak II Gneiss) crosscutting strongly deformed grey gneiss (Uivak I Gneiss). The *ca.* 3.75-3.70 Ga and *ca.* 3.6 Ga events were also recognized as xenocrysts in *ca.* 3.56 Ga monzonitic gneiss (Sałacińska et al. 2018), which therefore was intruded immediately after the formation of Uivak I Gneiss.

The protoliths of subsequent Paleoarchean gneisses formed during at least two unrelated magmatic events, at *ca.* 3.3 Ga and *ca.* 3.2 Ga. Emplacement of gneissic protoliths at 3.3 Ga was identified in this study, as well as by Krogh and Kamo (2006) and Komiya et al. (2017); (Fig. 8). The emplacement of gneissic protoliths at *ca.* 3.2 Ga has been identified as Lister Gneiss (Schiøtte et al. 1989a; Schiøtte et al. 1990). Both generations were grouped together as Lister Gneiss by Komiya et al. (2017). However, we distinguish these two generations on the basis of distinct ages and geochemistry.

The porphyroblastic gneiss collected from Maidmonts Island recorded an age of *ca.* 3.32 Ga (sample L1467). Gneisses with similar ages were also identified from the St John's Harbour (sample L1410), Nulliak Island and the adjacent coast (Komiya et al. 2017), and from Little Island (Krogh and Kamo 2006). All of these localities were mapped as Uivak II Gneiss in previous studies (Bridgwater et al. 1975; Hurst et al. 1975; Bridgwater and Collerson 1976; Collerson and Bridgwater 1979). Intrusive relationships between *ca.* 3.3 Ga and older (Uivak I) gneisses were recognized on Maidmonts Island (Fig. 3) and Little Island (Krogh and Kamo 2006). The latter study identified *ca.* 3.35 Ga orthogneiss (DB82.12; a deformed porphyritic granodiorite) that locally crosscut the foliation of the grey gneiss host. The host (DB82.74.1; a moderately layered tonalitic to granodioritic gneiss) was dated by Schiøtte et al. (1989a) at *ca.* 3.73 Ga, consistent with the protoliths of Uivak I Gneiss. The occurrence of xenocrysts with ages of *ca.* 3.76 Ga (LAD282; Komiya et al. 2017) and *ca.* 3.83-3.66 Ga (TK-89-5; Krogh and Kamo 2006) in *ca.* 3.3 Ga gneisses, as well as the geochemistry presented here (Fig. 5), indicate crustal involvement in the petrogenesis of this suite. Age equivalents of *ca.* 3.3 Ga granitic gneisses from the Saglek Block are unknown in south West Greenland (Næraa et al. 2012). The Uivak II Gneiss was originally correlated with the *ca.* 3.6 Ga iron-rich suite of Amîtsoq gneiss from the Nuuk region (Nutman et al. 1984), which contains a distinctive group of augen gneisses and ferrodiorites of mixed crustal and mantle origin. However, the new 3.3 Ga age disproves this correlation.

The TTG gneisses in this study include *ca.* 3.22 Ga trondhjemitic gneiss from Big Island (sample L1444), which has similar geochemical characteristics to the *ca.* 3.7 Ga TTG gneisses. A lack of intrusive relationships between the older Uivak and younger Lister gneisses and a lack of Eoarchean xenocrystic zircon in *ca.* 3.2 Ga Lister gneiss (Schiøtte et al. 1989a; Schiøtte et al. 1990; Wasteneys et al. 1996; Komiya et al. 2017; this study), as well as the geochemistry, is consistent with the hypothesis that the ca. 3.2 and ca. 3.7 Ga crustal rocks were not associated prior to late Archean tectonometamorphism, in contrast to ~~hypothesis~~ proposed by Bridgwater and Schiøtte (1991) and Wasteneys et al. (1996).

Following the model of Moyen (2011), the protoliths of the early Archean gneiss in the Saglek Block could have formed by partial melting of mafic crust under medium or high pressure conditions, with garnet and rutile, but no plagioclase, in the restite.

The presence of xenocrystic zircons (Fig. 6B,E), with ages comparable to parts of the Uivak I gneiss, ~~are~~ evidence of an additional, local crustal component. Trace element patterns of the orthogneisses from both the Saglek Block and south West Greenland are broadly similar, however individual samples display a different degree of REE fractionation (Fig. 5). Hoffman et al. (2011) has proposed a tectonic model involving re-melting of thickened island-arc crust in a vertical tectonic regime for the generation of medium pressure TTG. However, the higher pressure TTG with stronger REE fractionation patterns found in some Saglek samples bear a resemblance to *ca.* 3.7 Ga TTG in the Tarim Craton in northwestern China (Ge et al. 2018). According to Ge et al. (2018), the origin of high pressure TTG can be interpreted as a result of partial melting of a subducted proto-arc during arc accretion. Further investigation into the geochemistry of the Saglek Block will be needed to determine the relative importance of these petrogenetic scenarios.

9. Reassignment of units

Considering the ambiguity of the Uivak II Gneiss definition in previous literature, together with our new results presented here, we proposed a re-definition of gneissic nomenclature in the Saglek Block as follows:

Uivak Gneiss, previously called "early grey gneisses" (Bridgwater et al. 1975), "Uivak I gneiss" (Bridgwater and Collerson 1976) and "Uivak A-E Gneisses" (Komiya et al. 2017) is a diverse group of Eoarchean TTG gneisses whose protoliths formed in a series of unrelated magmatic events (Fig. 8), with some evidence of crustal reworking, and affected by at least one major period of deformation and metamorphism prior to intrusion of the Maidmonts Gneiss (formerly part of the 'Uivak II Gneiss'). This early Archean tectonothermal event occurred at *ca.* 3.6 Ga (Sałacińska et al. 2018 and references therein).

Maidmonts Gneiss, previously called "Uivak II augen gneiss" (Bridgwater and Collerson 1976) is a *ca.* 3.3 Ga crustally-contaminated granitoid that post-dates both formation of Eoarchean TTG gneisses and the *ca.* 3.6 Ga tectonothermal event (Fig. 8). It includes porphyritic and non-porphyritic granitoids intruded prior to metamorphism and deformation in the late Archean. The type area is on the western side of Maidmonts Island.

The previous definition of the **Lister Gneiss** (Schiøtte et al. 1989a) remains unchanged. This is a *ca.* 3.2 Ga granitoid gneiss (Fig. 8), occurring within Eoarchean Uivak Gneiss in the amphibolite-facies domain to the east of the Handy Fault. It is commonly indistinguishable in the field from Uivak Gneiss due to lack of intrusive relationships between these two units. The type locality is Lister Island. The 3.2-3.4 Ga gneisses grouped together by Komiya et al. (2017) as Lister Gneiss may in fact represent samples from both Lister and Maidmonts Gneiss.

Whilst our data do not preclude prolonged granitoid formation in the Eoarchean as suggested by Komiya et al. (2017), other published, more precise, zircon age data indicate that the formation of the Uivak Gneiss was, in fact, episodic.

10. Conclusions

Early Archean gneisses in the Saglek Block, previously called “Uivak I Gneiss”, represent different generations of magmatism over an interval between *ca.* 3.9 Ga and 3.6 Ga, with major magmatic events occurring between 3.75 Ga and 3.70 Ga, prior to tectonothermal activity at *ca.* 3.6 Ga. These include TTG gneisses with evidence of significant input resulting from crustal reworking, as indicated by xenocrystic zircon. Results show that the porphyroblastic gneisses on Maidmonts ~~Islands,~~ previously assigned to “Uivak II Gneiss”, were derived from a granite protolith emplaced after *ca.* 3.6 Ga tectonometamorphic event at *ca.* 3.3 Ga. Grey granitic gneisses of the same age and ~~geochemistry~~ are found elsewhere in the Saglek area and are considered to be co-genetic. We propose a re-definition of so-called “Uivak II Gneiss”, naming it “Maidmonts Gneiss”, after a type locality on Maidmonts Island. Lister Gneiss is a distinctive generation of tonalitic gneiss whose protolith formed at *ca.* 3.2 Ga, but with an unknown relationship to the older gneisses. Consequently, we define the Uivak ~~Gneissto represent~~ all TTG generated before the *ca.* 3.6 Ga tectonothermal event.

Acknowledgements

This research was conducted thanks to a grant to MAK by the Polish National Science Centre NCN (UMO 2014/15/B/ST10/04245), and grants to AS by SYNTHESYS (SE-TAF-6912) in the Swedish Museum of Natural History and an ING PAN internal project for young scientists. We also acknowledge grants to MJW from the Knut and Alice Wallenberg Foundation (2012.0097) and the Swedish Research Council (2012-4370). Fieldwork was carried out with the permission and support of Parks Canada and the Nunatsiavut Government. Special thanks to Darroch Whitaker and Martin Lougheed from Parks Canada and Rodd Laing form the Nunatsiavut Government for support in the field. The NordSIMS facility operates as Swedish/Icelandic infrastructure, of which this is publication ###.

References

Alderton DHM, Pearce JA, Potts PJ (1980) Rare earth element mobility during granite alteration: Evidence from southwest England. Earth Planet Sci Lett 49:149-165.

Baadsgaard H, Collerson KD, Bridgwater D (1979) The Archaean gneiss complex of northern Labrador. 1. Preliminary U–Th–Pb geochronology. Can. J. Earth Sci. 16(4):951-961.

Barker F (1979) Trondhjemites: definition, environment and hypothesis of origin. In: Barker F (Ed.), Trondhjemites, Dacites and Related Rocks. Elsevier, Amsterdam, 1-12.

Bridgwater D, Collerson KD (1976) The Major Petrological and Geochemical Characters of the 3,600 m.y. Uivak Gneisses from Labrador. Contrib. Mineral. Petrol. 54:43-59.

Bridgwater D, Collerson KD (1977) On the Origin of Early Archaean Gneisses: A Reply. Contrib. Mineral. Petrol. 62:179-191.

Bridgwater D, Collerson KD, Hurst RW, Jesscau CW (1975) Field characters of the early Precambrian rocks from Saglek, Coast of Labrador, Report of Activities. Department of Energy, Mines and Resources, Geological Survey of Canada, Ottawa, 287-296.

Bridgwater D, Schiøtte L (1991) The Archaean gneiss complex of Northern Labrador - A review of current results, ideas and problems. Bull. Geol. Soc. Denmark 39:153-166.

Bridgwater D, Watson J, Windley BF (1973) The Archaean craton of the North Atlantic region. Phil. Trans. Roy Soc. London A 273:493-512.

Chadwick B, Nutman AP (1979) Archaean structural evolution in the northwest Buksefjorden region S.W. Greenland. Precambrian Res. 9:199-226.

Collerson KD (1983) Ion microprobe zircon geochronology of the Uivak gneisses: implicaitons for the evolution of early terrestial crust in the North Atlantic Craton. Lunar and Planetary Institute Technical Report, Houston, Textas, 28-33.

Collerson KD, Bridgwater D (1979) Metamorphic development of early Archaean tonalitic and trondhjemitic gneisses: Saglek area, Labrador., in: Barker F (Ed.), Trondhjemites, Dacites, and Related Rock. Elsevier, Amsterdam, 205-271.

Collerson KD, Kerr A, Vocke RD, Hanson GN (1982) Reworking of sialic crust as represented in late Archaean-age gneisses, northern Labrador. Geology 10:202-208.

Condie KC (2005) TTGs and adakites: are they both slab melts? Lithos 80:33-44.

Condie KC, Sinha AK (1996) Rare earth and other trace element mobility during mylonitization: A comparison of the Brevard and Hope Valley shear zones in the Appalachian Mountains, USA. J Metamorph Geol 14:213-226.

Connelly JN and Ryan B (1996) Late Archean evolution of the Nain Province, Nain, Labrador: imprint of a collision. Can. J. Earth Sci. 33:1325-1342.

Crowley JL (2003) U-Pb geochronology of 3810–3630 Ma granitoid rocks south of the Isua greenstone belt, southern West Greenland. Precambrian Res. 126:235–257.

Drummond MS, Defant MJ (1990) A model from trondhjemite–tonalite–dacite genesis and crustal growth via slab melting: Archaean to modern comparisons. J Geophys Res 95:21503-21521.

Dunkley DJ, Kusiak MA, Wilde SA, Whitehouse MJ, Sałacińska A, Kielman R, Konečný P (submitted) Two Neoarchean orogenies on the western edge of the North Atlantic Craton, as revealed by SIMS dating of the Saglek Block, Nain Province, Labrador. J. Geol. Soc. Lond., submitted.

Fedo CM, Myers J, Appel PWU (2001) Depositional setting and paleogeographic implications of Earth's oldest supracrustal rocks, the> 3.7 Ga Isua Greenstone belt, West Greenland. Sedimentary Geology 141-142:61-77.

Foley S, Tiepolo M, Vanucci R (2002) Growth of early continental crust controlled by melting of amphibolite in subduction zones. Nature 417:837–840.

Friend CRL, Nutman AP (2005) Complex 3670–3500 Ma Orogenic Episodes Superimposed on Juvenile Crust Accreted between 3850 and 3690 Ma, Itsaq Gneiss Complex, Southern West Greenland. J Geol 113(4):375-397.

Ge R, Zhu W, Wilde SA, Wu H (2018) Remnants of Eoarchean continental crust derived from a subducted proto-arc. Sci. Adv. 4, eaao3159.

Greene BA (1974) Outline of geology of Labrador. Geosci. Can. 1(3):36-40.

Griffin WL, McGregor VR, Nutman AP, Taylor PN, Bridgwater D (1980) Early Archaean granulite-facies metamorphism south of Ameralik, West Greenland. Earth Planet. Sci. Lett. 50:59-74.

Hoffmann JE, Münker C, Næraa T, Rosing MT, Herwartz D, Garbe-Schönberg D, Svahnberg H (2011) Mechanisms of Archean crust formation inferred from high-precision HFSE systematic in TTGs. Geochim Cosmochim Acta 75:4157-4178.

Hoffman JE. Nagel TJ, Münker C, Næraa T, Rosing MT (2014) Constraining the process of Eoarchean TTG formation in the Itsaq Gneiss Complex, southern West Greenland. Earth and Planetary Science Letters 388:374-386.

Hölttä P, Balagansky V, Garde AA, Mertanen S, Peltonen P, Slabunov A, Sorjonen-Ward P, Whitehouse M (2008) Archean of Greenland and Fennoscandia. Episodes 31(1):13-19.

Hurst RW, Bridgwater D, Collerson KD, Wetherill GW (1975) 3600 m.y. Rb-Sr ages from very early Archaean gneisses from Saglek Bay, Labrador. Earth Planet. Sci. Lett. 27:393-403.

Irvine TN, Baragar WRA (1971) A guide to the chemical classification of the common volcanic rocks. Can. J. Earth Sci. 8:523-548.

Jahn B, Glikson AY, Peucat JJ, Hickman AH (1981) REE geochemistry and isotopic data of Archaean silicic volcanics and granitoids from the Pilbara block, western Australia: implications for early crustal evolution. Geochim Cosmochim Acta 45:1633-1652.

Janoušek V, Moyen JF, Martin H, Erban V, Farrow C (2016) Geochemical Modelling of Igneous Processes – Principles And Recipes in R Language. Springer Geochemistry.

Jeon H, Whitehouse MJ (2015) A Critical Evaluation of U-Pb Calibration Schemes Used in SIMS Zircon Geochronology. Geostand. Geoanal. Res. 39:443-452.

Kamber BS, Ewart A, Collerson KD, Bruce M, McDonald GD (2002) Fluid-mobile trace element constraints on the role of slab melting and implications for Archaean crustal growth models. Contrib. Mineral. Petrol. 144:38-56.

Komiya T, Yamamoto S, Aoki S, Koshida K, Shimojo M, Sawaki Y, Aoki K, Sakata S, Yokoyama TD, Maki K, Ishikawa A, Hirata T, Collerson KD (2017) A prolonged granitoid formation in Saglek Block, Labrador: Zonal growth and crustal reworking of continental crust in the Eoarchean. Geoscience Frontiers 8:355-385.

Komiya T, Yamamoto S, Aoki S, Sawaki Y, Ishikawa A, Tashiro T, Koshida K, Shimojo M, Aoki K, Collerson KD (2015) Geology of the Eoarchean, >3.95 Ga, Nulliak supracrustal rocks in the Saglek Block, northern Labrador, Canada: The oldest geological evidence for plate tectonics. Tectonophysics 662:40-66.

Krogh TE, Kamo SL (2006) Precise U-Pb zircon ID-TIMS ages provide an alternative interpretation to early ion microprobe ages and new insights into Archean crustal processes, northern Labrador, in: Reimold, W.U., Gibson, R.L. (Eds.), Processes on the Early Earth: Geol. Soc. Spec. Pap. 91-103.

Kusiak MA, Dunkley DJ, Whitehouse MJ, Wilde SA, Sałacińska A, Konečný P, Szopa K, Gawęda A, Chew D (2018) Peak to post-peak thermal history of the Saglek Block of Labrador: a multiphase and multi-instrumental approach to geochronology. Chem Geol. 484:210-223.

Ludwig KR (2012) Isoplot 3.75: A geochronological toolkit for Microsoft Excel. Berkeley Geochronology Center Special Publication 5.

Martin H (1987) Petrogenesis of Archaean trondhjemites, tonalites and granodiorites from eastern Finland; major and trace element geochemistry. J. Petrol. 28:921-953.

Martin H (1993) The mechanisms of petrogenesis of the Archean continental crust-comparison with modern processes. Lithos 30:373-388.

Martin H, Smithies RH, Rapp RP, Moyen JF, Champion DC (2005) An overview of adakite, tonalite–trondhjemite–granodiorite (TTG) and sanukitoid: relationships and some implications for crustal evolution. Lithos 79:1-24.

McDonough W, Sun SS (1995) The composition of the Earth. Chem Geol. 67(5):1050-1056

McGregor VR (1973) The early Precambrian gneisses of the Godthåb district, West Greenland: Philos. Trans. Royal Soc. A A273:343–358.

McGregor VR, Mason B, (1977) Petrogenesis and geochemistry of metabasaltic and metasedimentary enclaves in the Amiıtsoq gneisses, West Greenland. Am. Mineral. 62:887-904.

Middlemost E (1994) Naming materials in the magma/igneous rock system. Earth Science Reviews 37: 215-224.

Moyen JF (2011) The composite Archaean grey gneisses: petrological significance, and evidence for a non-unique tectonic setting for Archaean crustal growth. Lithos 123:21-36.

Moyen JF, Stevens G (2006) Experimental constraints on TTG petrogenesis: implications for Archean geodynamics. In: Benn K, Mareschal JC, Condie KC (Eds.), Archean geodynamics and environments. Monographs. AGU, 149-178.

Næraa T, Scherstén A, Kemp AIS, Rosing MT, Hoffmann JE, Kokfelt TF, Whitehouse MJ, (2012) Hafnium isotope evidence for a transition in the dynamics of continental growth 3.2 Gyr ago. Nature 485:627–631.

Nutman AP, Bennett VC, Friend CRL, Hidaka H, Yi K, Lee SR, Kamiichi T (2013) The Itsaq Gneiss Complex of Greenland: Episodic 3900 to 3660 Ma juvenile crust formation and recycling in the 3660 to 3600 Ma Isukasian orogeny: Am. J. Sci. 313(9):877–911.

Nutman AP, Bennett VC, Friend CRL, Norman MD (1999) Meta-igneous (non-gneissic) tonalites and quartz-diorites from an extensive ca. 3800 Ma terrain south of the Isua supracrustal belt, southern West Greenland: constraints on early crust formation. Contrib. Mineral. Petrol. 137:364-388.

Nutman AP, Bridgwater D, Fryer B (1984) The iron rich suite from the Amitsoq gneisses of southern West Greenland: Early Archaean plutonic rocks of mixed crustal and mantle origin. Contrib. Mineral. Petrol. 87:24-34.

Nutman AP, Friend CRL (2007) Adjacent terranes with ca. 2715 and 2650 Ma high-pressure metamorphic assemblages in the Nuuk region of the North Atlantic Craton, southern West Greenland: Complexities of Neoarchaean collisional orogeny. Precambrian Res. 155:159-203.

Nutman AP, Friend CRL, Barker SS, McGregor VR (2004a) Inventory and assessment of Palaeoarchaean gneiss terrains and detrital zircons in southern West Greenland. Precambrian Res. 135:281-314.

Nutman AP, Friend CRL, Bennett VC, McGregor VR (2000) The early Archaean Itsaq Gneiss Complex of southern West Greenland: the importance of field observations in interpreting dates and isotopic data constraining early terrestrial evolution. Geochim. Cosmochim. Acta 64:3035-3060.

Nutman AP, Friend CRL, Bennett VC (2002) Evidence for 3650–3600 Ma assembly of the northern end of the Itsaq Gneiss Complex, Greenland: implication for early Archean tectonics. Tectonics 21(5):15-28.

Nutman AP, Friend CRL, Bennett VC, McGregor VR (2004b) Dating of the Ameralik dykes of the Nuuk district, Greenland: multiple intrusion events starting from ca. 3510 Ma. J. Geol. Soc. Lond. 161:421-430.

Nutman AP, Friend CRL, Horie K, Hidaka H (2007) Te Itsaq Gneiss Complex of Southern West Greeland and the Construction of Eoarchaean Crust at Convergent Plate Boundaries. In Kranendonk M, Smithies R, Bennet VC (Eds.), Earth's oldest rocks (187-218). Amsterdam: Elsevier BV.

Nutman AP, McGregor VR, Friend CRL, Bennett VC, Kinny PD (1996) The Itsaq Gneiss Complex of southern west Greenland, the world's most extensive record of early crustal evolution (3900-3600 Ma), Precambrian Res. 78:1-39.

O'Connor JT (1965) A classification for quartz-rich igneous rocks based on feldspar ratios. In: US Geological Survey Professional Paper B525. USGS, 79-84.

Polat A, Hofmann AW (2003) Alteration and geochemical patterns in the 3.7–3.8 Ga Isua greenstone belt, West Greenland. Precambrian Res. 126:197-218.

Polat A, Frei R, Scherstén A, Appel PWU (2010) New age (ca. 2970 Ma), mantle source composition and geodynamic constraints on the Archean Fiskenæsset anorthosite complex, SW Greenland. Chem. Geol. 277:1–20.

Rapp RP, Shimizu N, Norman MD (2003) Growth of early continental crust by partial melting of eclogite. Nature 425:605-609.

Rapp RP, Watson EB, Miller CF (1991) Partial melting of amphibolite/eclogite and the origin of Archaean trondhjemites and tonalites. Precambrian Res. 51:1-25.

Regelous M, Collerson KD (1996) 147Sm-143Nd, 146Sm-142Nd systematics of Early Archaean rocks and implications for crust-mantle evolution. Geochim. Cosmochim. Acta 60:3513-3520.

Ryan B, Martineau Y (2012) Revised and coloured edition of 1992 map showing the Geology of the Saglek Fiord - Hebron Fiord area, Labrador (NTS 14L/2,3,6,7). Scale: 1:100 000, Government of Newfoundland and Labrador, Department of Natural Resources, Geological Survey, Map 2012-2015, Open File 2014L/0091 (Update of map originally released as Newfoundland Department of Mines and

Energy, Geological Survey Branch, Map 2092-2018B and Geological Survey of Canada, Open File 2466).

Sałacińska A, Kusiak MA, Whitehouse MJ, Dunkley DJ, Wilde SA, Kielman R (2018) Complexity of the early Archean Uivak Gneiss: Insights from Tigigagkyuk Inlet, Saglek Block, Labrador, Canada and possible correlations with south West Greenland. Precambrian Res. 315:103-119.

Schiøtte L, Compston W, Bridgwater D (1989a) Ion-probe U-Th-Pb zircon dating of polymetamorphic orthogneisses from northern Labrador, Canada. Can. J. Earth Sci. 26:1533-1556.

Schiøtte L, Compston W, Bridgwater D (1989b) U-Th-Pb ages of single zircons in Archean supracrustals from Labrador, Canada. Can. J. Earth Sci. 26:2636-2644.

Schiøtte L, Noble S, Bridgwater D (1990). U-Pb mineral ages from northern Labrador: Possible evidence for interlayering of Early and Middle Archean tectonic slices. Geosci. Can. 17(4):227-231.

Shand SJ (1943) Eruptive Rocks. Their Genesis, Composition, Classification, and Their Relation to Ore-Deposits with a Chapter on Meteorite. New York: John Wiley & Sons.

Shimojo M, Yamamoto S, Sakata S, Yokoyama TD, Maki K, Sawaki Y, Ishikawa A, Aoki K, Aoki S, Koshida K, Tashiro T, Hirata T, Collerson KD, Komiya T (2016) Occurrence and geochronology of the Eoarchean, ~3.9 Ga, Iqaluk Gneiss in the Saglek Block, northern Labrador, Canada: Evidence for the oldest supracrustal rocks in the world. Precambrian Res. 278, 218-243.

Stacey JS, Kramers JD (1975) Approximation of terrestrial lead isotope evolution by a two-stage model. Earth Planet. Sci. Lett. 26:207-221.

Taylor FC (1971) A revision of Precambrian structural provinces in northeastern Quebec and northern Labrador. Can. J. Earth Sci. 8(5), 579-584.

Wanless RK, Bridgwater D, Collerson KD (1979) Zircon age measurements for Uivak II gneisses from the Saglek area, Labrador. Can. J. Earth Sci. 16:962-965.

Ward CD, McArthur JM, Walsh JN (1992) Rare Earth Element Behaviour During Evolution and Alteration of the Dartmoor Granite, SW England. J. Petrol. 33:785-815.

Wardle RJ, Gower CF, Ryan B, Nunn GA, James DT, Kerr A (1997) Geological Map of Labrador: 1:1 million scale. Government of Newfoundland and Labrador, Department of Mines and Energy, Geological Survey, Map 97-07.

Wasteneys HA, Wardle RJ, Krogh TE (1996) Extrapolation of tectonic boundaries across the Labrador shelf: U-Pb geochronology of well samples: Can. J. Earth Sci. 33, 1308-1324.

Whitehouse MJ, Kamber BS (2005) Assigning dates to thin gneissic veins in high-grade metamorphic terranes: A cautionary tale from Akilia, southwest Greenland. J. Petrol. 46, 291-318.

Whitehouse MJ, Kamber BS, Moorbath S (1999) Age significance of U-Th-Pb zircon data from early Archaean rocks of west Greenland - a reassessment based on combined ion-microprobe and imaging studies. Chem. Geol. 160:201-224.

Wiedenbeck M, Alle P, Corfu F, Griffin WL, Meier M, Oberli F, Vonquadt A, Roddick JC, Speigel W (1995) 3 Natural Zircon Standards for U-Th-Pb, Lu-Hf, Trace-Element and Ree Analyses. Geostandard Newslett, 19:1-23.

Zeck HP, Whitehouse MJ (1999) Hercynian, Pan-African, Proterozoic and Archean ion-microprobe zircon ages for a Betic-Rif core complex, Alpine belt, W Mediterranean - consequences for its P-T-t path. Contrib. Mineral. Petr. 134:134-149.

Figures:

Figure 1. Geological map of northeast Labrador from Ramah Bay to Hebron Fjord, modified after Wardle et al. (1997). Sample locations for this and previous studies are represented by symbols: 1 – Schiøtte et al. (1989a); 2 – Krogh and Kamo (2006); 3 – Komiya et al. (2017); 4 – Shimojo et al. (2016); 5 – Kusiak et al. (2018); 6 – Sałacińska et al. (2018); 7 – Dunkley et al. (submitted); 8 – Wasteneys et al. (1996).

Figure 2. Sample localities of gneisses in the Saglek Block: A – homogenous fine-grained gneiss L1410 from St John's Harbour; B – banded grey gneiss L1411 from St John's Harbour; C – weakly pophyroblastic gneiss L1443 from Big Island; D – homogenous fine-grained gneiss L1444 from Big Island; E – grey gneiss (L1463) cut by segmented mafic dyke and intruded by syn-tectonic granite, which is deformed into a late gniessosity that transposes the earlier gneissosity on Little Island; F – deformed and transposed contacts between porphyroclastic gneiss (L1467), grey gneiss and granitoid on Maidmonts Island.

Figure 3. A – Geological map of Maidmonts Island showing sample location modified after Ryan and Martineau (2012). B – location of porphyroclastic gneiss, which intrudes earlier gneissosity in strongly laminated pale grey gneiss on Maidmonts Island. All gneisses are cut by K-feldspar-rich pegmatite and granodioritic dyke. C – location of intrusive relationship between originally porphyritic granite and fine-grained grey gneisses on the west coast of Maidmonts Island. Porphyroclastic gneiss intrudes strongly laminated pale grey gneiss. Green line – fault; red line – intrusive contact between Uivak I and Uivak II; blue line – granitic to granodioritic dykes intruded along faults.

Figure 4. Major element diagrams for the grey gneisses from the Saglek Block. A – total alkali versus silica (TAS) diagram (Middlemost 1994); B – A/CNK vs A/NK plot of Shand (1943); C – AFM diagram (Irvine and Baragar 1971), $Na_2O + K_2O$ (A), Fe_2O_3*=total Fe expressed as Fe_2O_3 (F), and MgO (M); D – An–Ab–Or triangle (Barker 1979; after O'Connor 1965). Data from previous studies are from Collerson and Bridgwater (1979); Schiøtte et al. (1989a) and Sałacińska et al. (2018). Data for Færingehavn and Isukasia terranes in West Greenland from Nutman et al. (1996, 1999, 2007), Kamber et al. (2002), Næraa et al. (2012) and Hoffman et al. (2011, 2014).

Figure 5. Trace element diagrams for grey gneisses in the Saglek Block. A - Primitive mantle-normalized diagram. B – $(La/Yb)_N$ vs. Yb_N diagram (modified after Martin 1993, and Condie 2005). C – Chondrite-normalized REE diagram. Normalization values from McDonough and Sun (1995). Data for Tigigakyuk Inlet are from Sałacińska et al. (2018); for West Greenland from Nutman et al. (1996, 1999, 2007), Kamber et al. (2002), Næraa et al. (2012), Hoffman et al. (2011, 2014), and for Tarim Craton in North-west China from Ge et al. (2018).

Figure 6. CL images of zircons from: A – sample L1410; B – sample L1411; C – sample L1443; D – sample L1444; E – sample L1463; F – sample L1467. Ages ($^{207}Pb/^{206}Pb$); c – high common Pb (>1%); d – discordant (>5%); m – mixture of growth zones.

Figure 7. SIMS zircon analyses using Tera-Wasserburg plots; A – L1410; B – L1411; C – L1443; D – L1444; E – L1463; F – L1467. Black ellipse – concordant data (<5%); grey ellipse – discordant data (>5%); dashed ellipse - high common Pb data (>1%); analyses of mixed zones are not shown. All data-point error ellipses are 2σ.

Figure 8. Summary of U-Pb zircon age determinations of gneisses from the Saglek Block in Labrador. Data sources: 1 – this study; 2 – Sałacińska et al. (2018); 3 – Kusiak et al. (2018); 4 – Dunkley et al. (submitted); 5 – Schiøtte et al. (1989a); 6 – Wasteneys et al. (1996); 7 – Schiøtte et al. (1990); 8 – Krogh and Kamo (2006); 9 – Komiya et al. (2017); 10 – Shimojo et al. (2016).

Figure

Click here to download Figure Salacinska et al. FIG.1.pdf

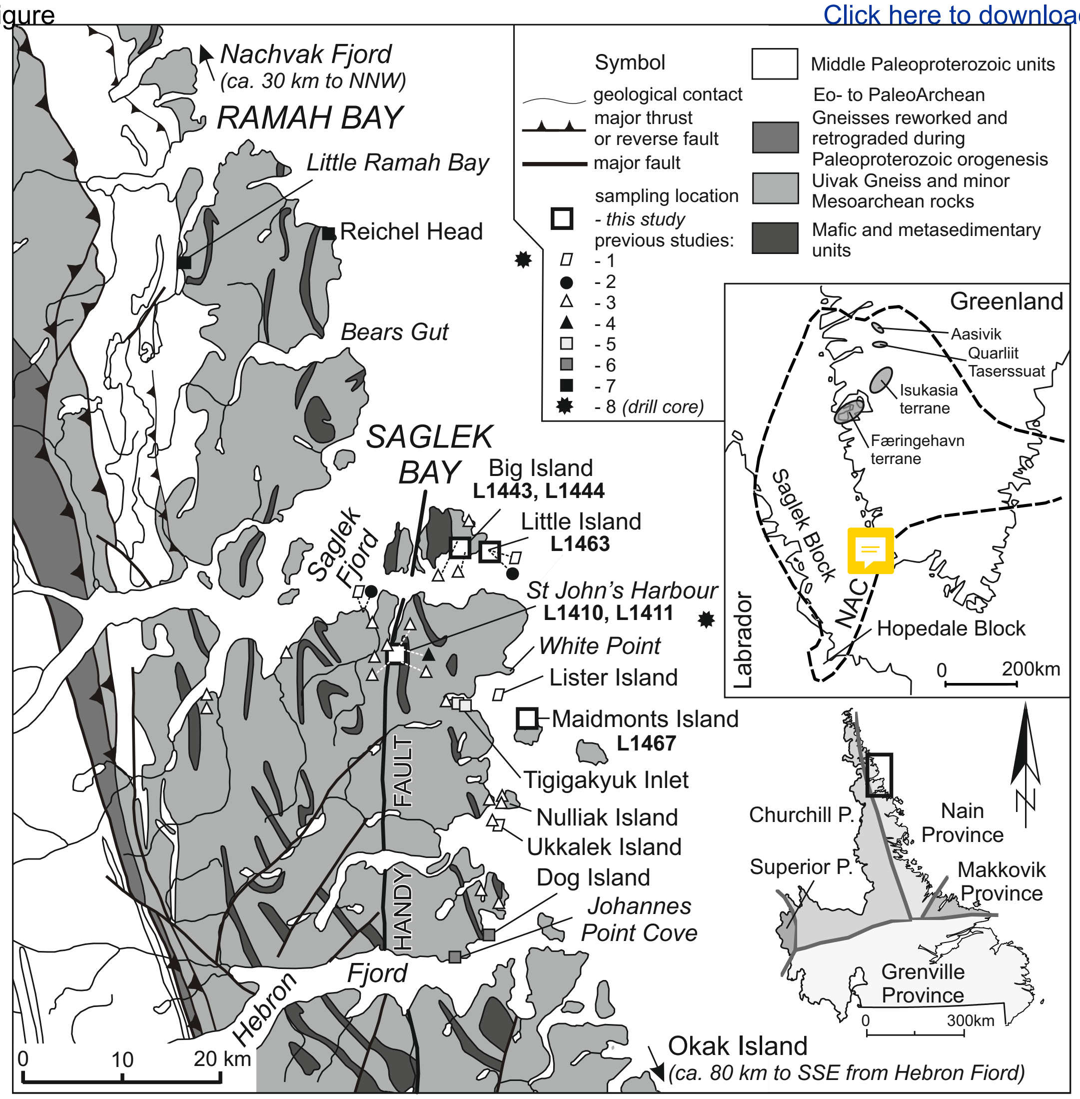

Figure

Click here to download Figure Salacinska et al. FIG.2.pdf

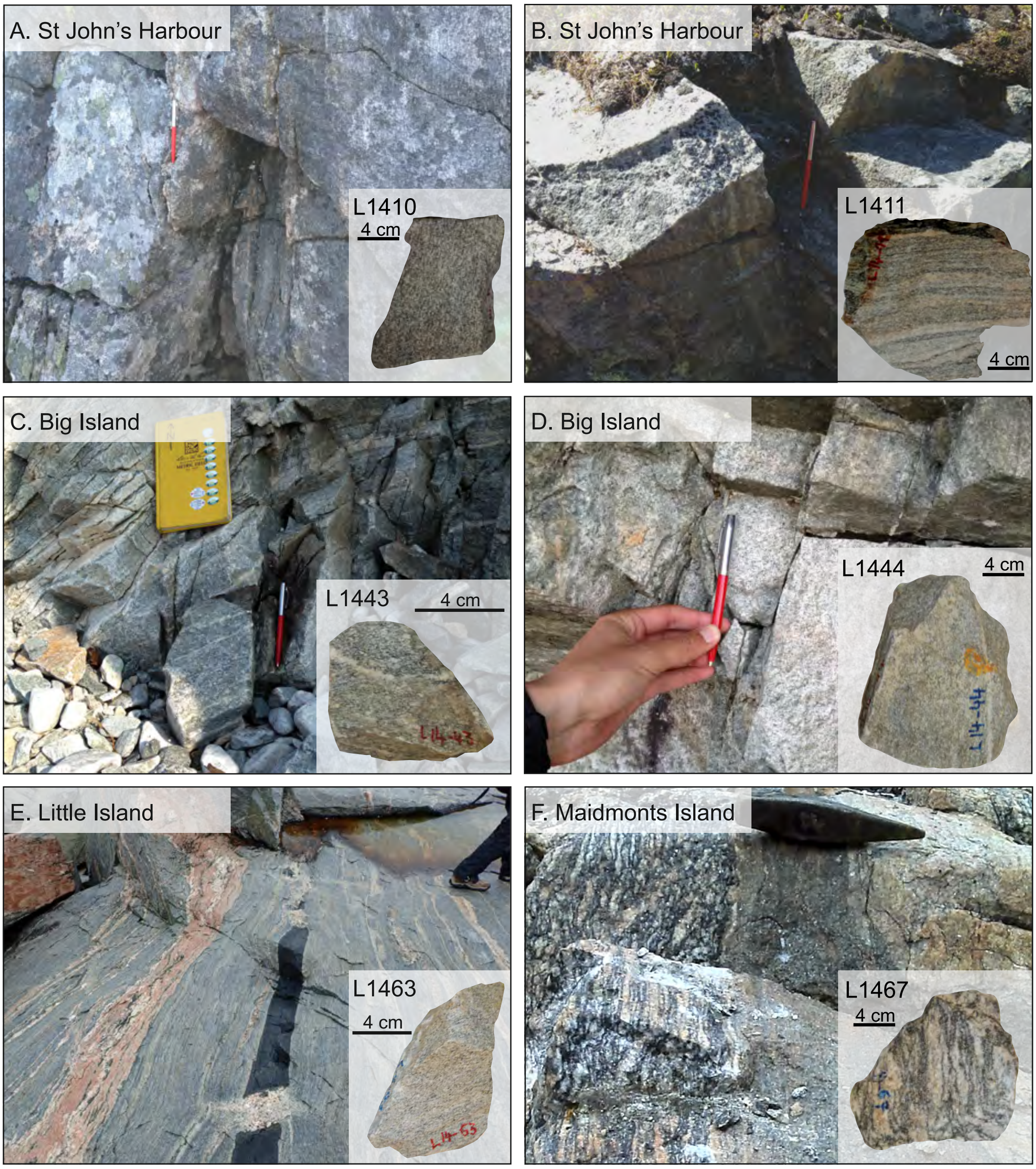

Figure

Click here to download Figure Salacinska et al. FIG.3.pdf

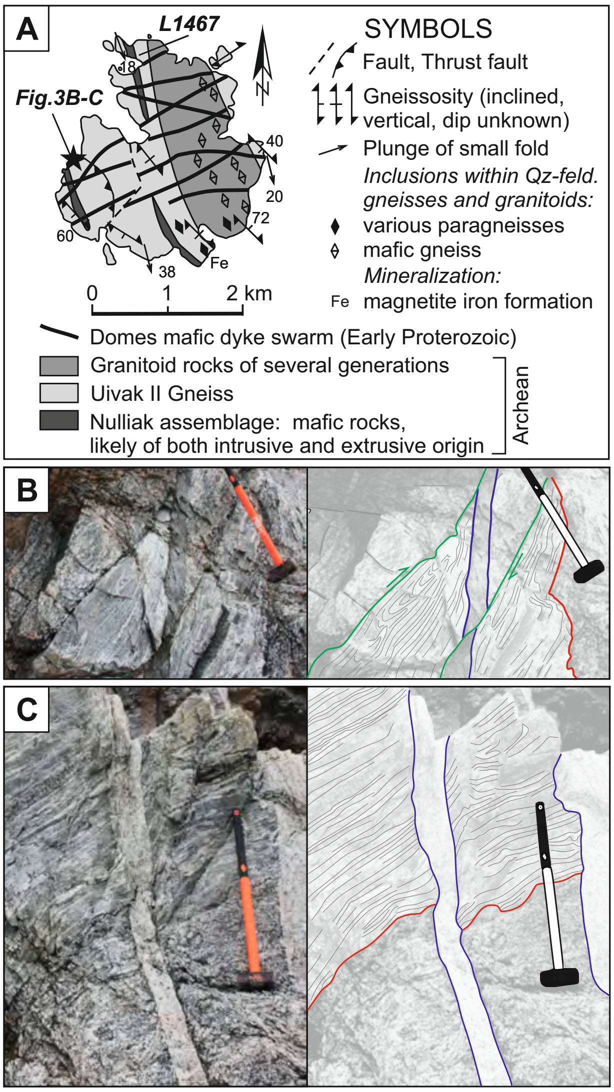

Figure

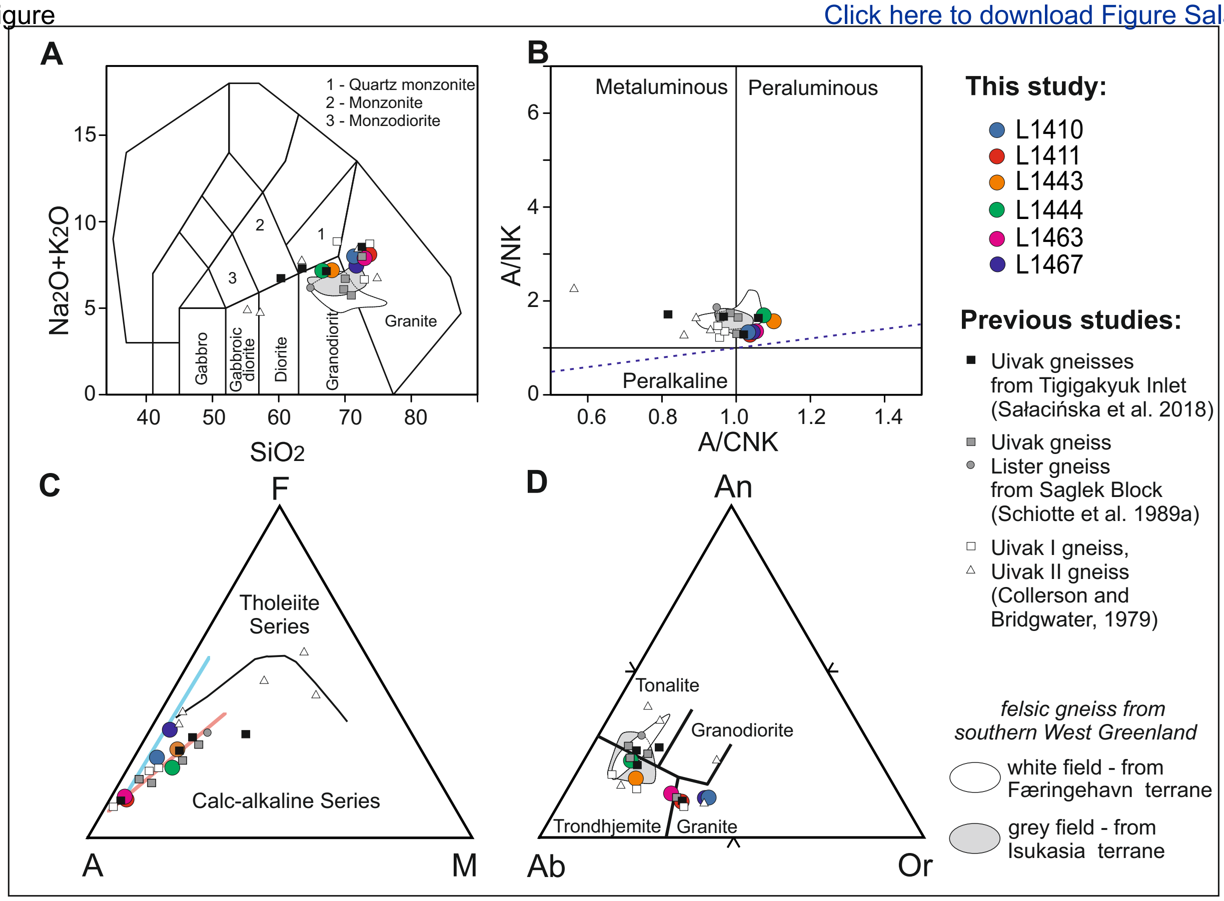
A
1 - Quartz monzonite
2 - Monzonite
3 - Monzodiorite
Gabbro
Gabbroic diorite
Diorite
Granodiorite
Granite
Na2O+K2O
SiO2
B
Metaluminous
Peraluminous
Peralkaline
A/NK
A/CNK
C
F
Tholeiite Series
Calc-alkaline Series
A
M
D
An
Tonalite
Granodiorite
Trondhjemite
Granite
Ab
Or
This study:
L1410
L1411
L1443
L1444
L1463
L1467
Previous studies:
Uivak gneisses from Tigigakyuk Inlet (Sałacińska et al. 2018)
Uivak gneiss
Lister gneiss from Saglek Block (Schiotte et al. 1989a)
Uivak I gneiss,
Uivak II gneiss (Collerson and Bridgwater, 1979)
felsic gneiss from southern West Greenland
white field - from Færingehavn terrane
grey field - from Isukasia terrane

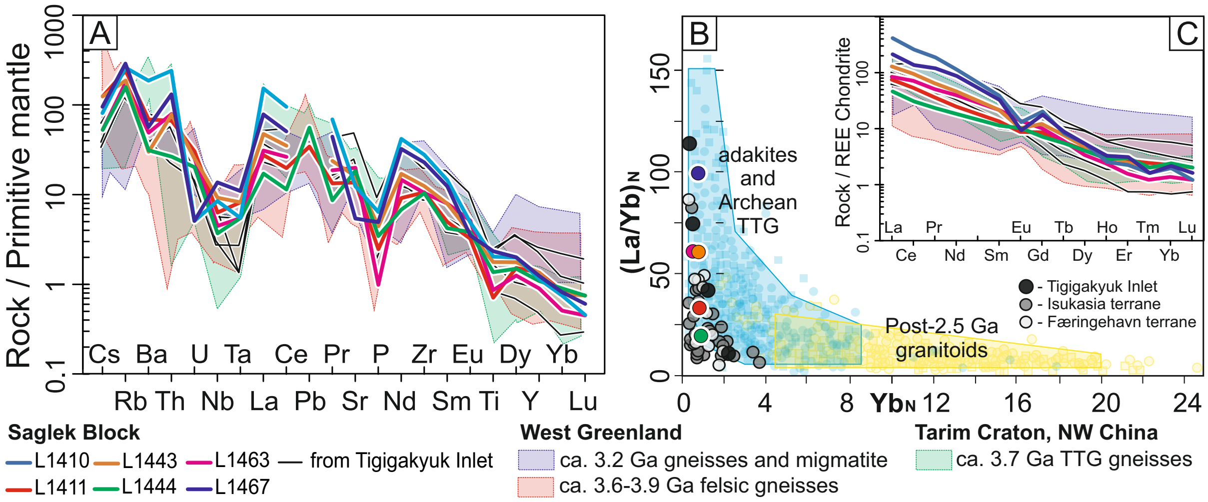
A
Rock / Primitive mantle
0.1
1
10
100
1000
Cs Ba U Ta Ce Pr P Zr Eu Dy Yb
Rb Th Nb La Pb Sr Nd Sm Ti Y Lu
B
(La/Yb)N
0
50
100
150
adakites and Archean TTG
Post-2.5 Ga granitoids
0 4 8 YbN 12 16 20 24
C
Rock / REE Chondrite
0.1
1
10
100
La Pr Eu Tb Ho Tm Lu
Ce Nd Sm Gd Dy Er Yb
- Tigigakyuk Inlet
- Isukasia terrane
- Færingehavn terrane
Saglek Block
L1410 L1443 L1463 — from Tigigakyuk Inlet
L1411 L1444 L1467
West Greenland
ca. 3.2 Ga gneisses and migmatite
ca. 3.6-3.9 Ga felsic gneisses
Tarim Craton, NW China
ca. 3.7 Ga TTG gneisses

Figure

Click here to download Figure Salacinska et al. FIG.6.pdf

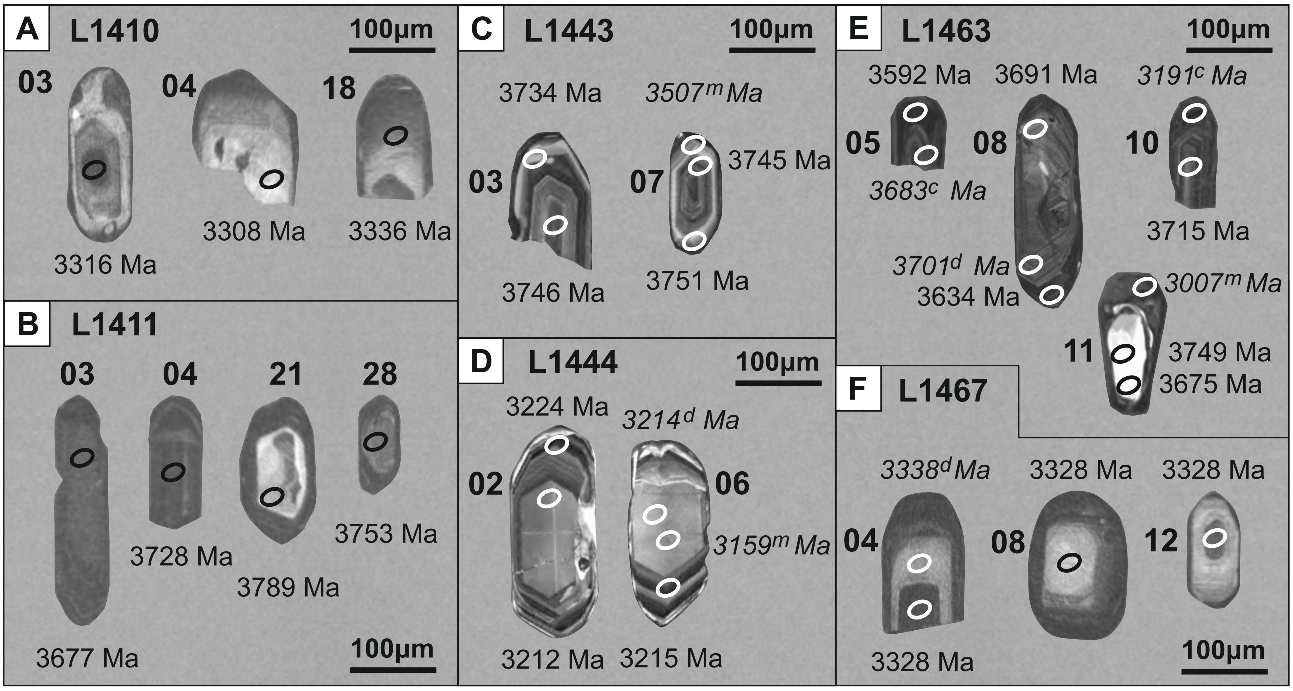

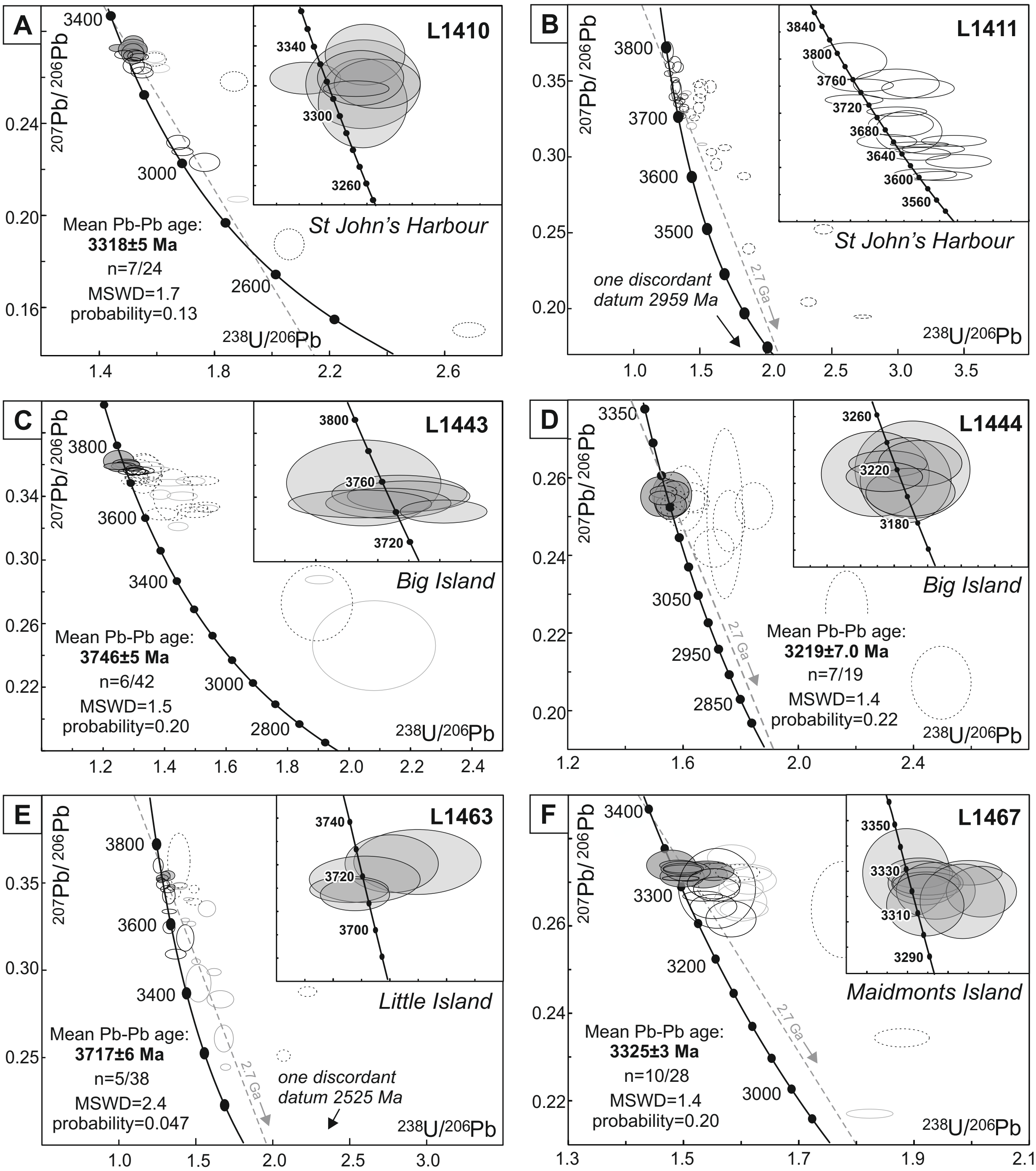
A
L1410
St John's Harbour
Mean Pb-Pb age:
3318±5 Ma
n=7/24
MSWD=1.7
probability=0.13
B
L1411
St John's Harbour
one discordant
datum 2959 Ma
2.7 Ga
C
L1443
Big Island
Mean Pb-Pb age:
3746±5 Ma
n=6/42
MSWD=1.5
probability=0.20
D
L1444
Big Island
Mean Pb-Pb age:
3219±7.0 Ma
n=7/19
MSWD=1.4
probability=0.22
2.7 Ga
E
L1463
Little Island
Mean Pb-Pb age:
3717±6 Ma
n=5/38
MSWD=2.4
probability=0.047
one discordant
datum 2525 Ma
2.7 Ga
F
L1467
Maidmonts Island
Mean Pb-Pb age:
3325±3 Ma
n=10/28
MSWD=1.4
probability=0.20
2.7 Ga
207Pb/206Pb
238U/206Pb

Figure

Click here to download Figure Salacinska et al. FIG.8.pdf

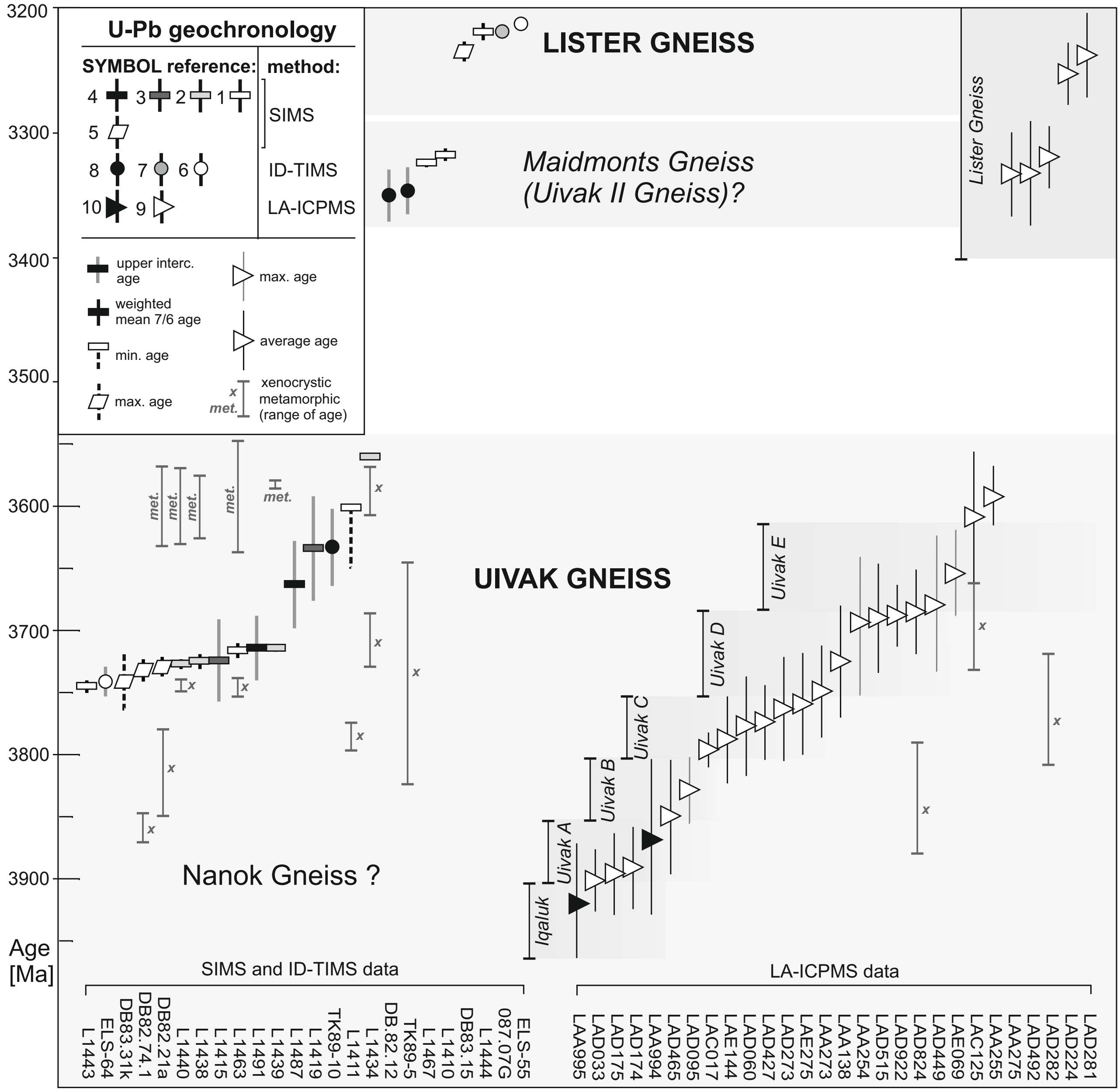

Table 1. Sample locations and modal mineral assemblages

Sample	Type	locality	latitude	longitude	Qz	Pl	Afs	Hbl	Bt	Py	Chl	Ser	Ep	Zrn	Ap
L1410	granitic orthogneiss	St John's Harbour	58°26,76´N	62°47,53´W	•••	•••	••		••		2^{o}	2^{o}	2^{o}	•	•
L1411	granitic orthogneiss	St John's Harbour	58°26,76´N	62°47,43´W	•••	•••	••		••		2^{o}	2^{o}		•	•
L1443	trondhjemitic orthogneiss	Big Island	58°32,55´N	62°40,60´W	•••	•••	••		••		2^{o}	2^{o}		•	•
L1444	trondhjemitic orthogneiss	Big Island	58°32,79´N	62°41,07´W	•••	•••	••	••	••		2^{o}	2^{o}		•	•
L1463	trondhjemitic orthogneiss	Little Island	58°32,06´N	62°38,64´W	•••	•••	•••		••		2^{o}	2^{o}	2^{o}	•	•
L1467	granitic orthogneiss	Maidmonts Island	58°23,28´N	62°33,55´W	•••	•••	••		••	••	2^{o}	2^{o}	2^{o}	•	•

major (•••), minor (••) and accessory (•) amounts, (2^{o}) secondary mineral. Qz, quartz; Pl, plagioclase; Afs, alkali feldspar; Hbl, hornblende; Bt, biotite; Py, pyrite; Chl, chlorite; Ser, sericite; Ep, epidote; Zrn, zircon; Ap, apatite.

Table 2. Whole-rock major and trace element compositions of gneisses from the Saglek Block

sample	L1410	L1411	L1443	L1444	L1463	L1467
SiO_2	70.81	73.7	66.53	66.00	72.26	71.22
TiO_2	0.40	0.14	0.35	0.27	0.17	0.46
Al_2O_3	14.37	14.6	16.61	18.5	15.13	13.54
Fe_2O_3	3.09	1.28	3.33	2.48	1.31	4.31
MnO	0.03	0.02	0.03	0.03	0.02	0.05
MgO	0.67	0.45	1.17	1.19	0.37	0.61
CaO	1.76	1.51	2.49	3.49	1.79	1.60
Na_2O	3.79	4.53	5.17	5.66	4.65	3.62
K_2O	4.13	3.56	1.87	1.43	3.17	3.77
P_2O_5	0.13	0.05	0.09	0.07	0.02	0.10
LOI	0.60	0.26	2.20	1.21	1.00	0.60
Cs	1.7	2.6	2.6	1.1	1.1	2.0
Rb	157	144	112	94	106	174
Ba	1232	451	196	204	321	372
Nb	5.5	4.1	6.0	2.4	2.9	8.9
Ta	0.2	0.3	0.3	0.2	0.2	0.4
Sr	244	269	316	362	392	106
Zr	290	110	129	108	108	238
Y	4.8	5.7	5.7	4.6	3.8	5.2
Hf	7.2	3.3	3.5	2.6	3.6	6.3
Ni	<20	1.4	<20	9.2	<20	<20
V	22	18	37	37	17	30
Pb	n.a.	5.1	n.a.	8.3	n.a	n.a.
U	0.1	0.6	0.5	0.4	0.5	0.1
Th	19.3	5.3	6.2	2.1	6.3	10.5
La	99.10	17.70	30.50	11.00	19.90	50.70
Ce	159.4	32.7	58.2	18.9	43.7	84.5
Pr	17.46	3.35	5.97	2.17	4.69	11.18
Nd	52	11.3	21.1	8.4	18.1	40.1
Sm	5.82	1.99	3.18	1.69	3.19	4.96
Eu	0.74	0.49	0.57	0.58	0.78	0.53
Gd	4.07	1.7	2.41	1.43	2.02	3.55
Tb	0.30	0.21	0.28	0.20	0.22	0.32
Dy	1.31	1.01	1.17	0.99	0.83	1.32
Ho	0.14	0.16	0.18	0.16	0.13	0.18
Er	0.36	0.43	0.39	0.48	0.25	0.5
Tm	0.04	0.06	0.05	0.05	0.03	0.04
Yb	0.32	0.36	0.34	0.39	0.22	0.35
Lu	0.03	0.05	0.05	0.05	0.03	0.04
K_2O/Na_2O	1.09	0.79	0.36	0.25	0.68	1.04
La/Yb	309.7	49.2	49.2	28.2	90.5	144.9
Eu/Eu*	0.46	0.81	0.63	1.14	0.94	0.39

Table 3. SIMS U-Th-Pb data for sample L1410, n5691 from St John's Harbour

Sample[1]	U	Th	Pb	Th/U	$f^{206}Pb$[2]	Disc. %	Ratios[3]				Ages[3]			
spot #	ppm	ppm	ppm		%		$^{238}U/^{206}Pb$	±σ (%)	$^{207}Pb/^{206}Pb$	±σ (%)	$^{207}Pb/^{206}Pb$	±σ	$^{206}Pb/^{238}U$	±σ
n5691-18c	66	30	60.8	0.43	0.05	-2.8	1.5183	0.95	0.275125	0.45	3335	7	3262	24
n5691-10c	42	27	40.2	0.61	{0.02}	-2.1	1.5143	1.03	0.272785	0.41	3322	6	3269	26
n5691-09c	130	104	131.2	0.81	0.06	1.2	1.4654	0.87	0.272767	0.24	3322	4	3354	23
n5691-06c2	52	38	49.7	0.73	{0.03}	-2.9	1.5291	1.02	0.272206	0.37	3319	6	3244	26
n5691-05c	27	17	25.7	0.61	{0.07}	-2.1	1.5166	1.37	0.272157	0.67	3318	10	3265	35
n5691-03c	622	604	630.0	0.96	0.15	-1.6	1.5104	0.79	0.271711	0.12	3316	2	3275	20
n5691-04c	37	19	34.2	0.52	{0.02}	-1.6	1.5163	1.06	0.270256	0.68	3308	11	3265	27
n5691-13c	87	72	87.1	0.82	{0.01}	0.5	1.4849	0.87	0.269973	0.28	3306	4	3319	23
n5691-16c	50	38	48.2	0.75	{0.02}	-1.8	1.5208	0.98	0.269540	0.38	3303	6	3258	25
n5691-07r	98	57	91.1	0.57	0.08	-2.4	1.5303	0.85	0.269434	0.34	3303	5	3242	22
n5691-14r	140	72	127.9	0.51	0.04	-2.8	1.5386	0.86	0.268936	0.23	3300	4	3228	22
n5691-17c	104	75	99.5	0.72	0.05	-0.7	1.5194	0.99	0.265118	0.55	3277	9	3260	25
n5691-20c	51	32	47.3	0.63	{0.05}	-2.1	1.5453	0.98	0.263970	0.38	3271	6	3217	25
n5691-15c	61	40	56.7	0.65	{0.02}	-1.9	1.5490	1.02	0.262144	0.37	3260	6	3211	26
n5691-21c1	53	52	47.5	0.96	{0.05}	-1.8	1.6739	0.98	0.231761	0.55	3064	9	3019	24
n5691-01c	97	51	78.1	0.50	0.06	-1.6	1.6888	0.90	0.227751	0.32	3036	5	2998	22
n5691-21c2	39	38	32.7	0.97	0.07	-4.6	1.7655	1.23	0.223141	0.73	3003	12	2893	29
>5% disc.														
n5691-19c	53	30	47.5	0.51	0.08	-6.0	1.5916	0.94	0.268938	0.38	3300	6	3143	23
n5691-06c1	90	52	79.2	0.54	0.26	-5.6	1.6027	1.07	0.264031	0.31	3271	5	3126	27
n5691-11c	590	7	378.8	0.01	0.18	-5.8	1.8816	0.79	0.207074	0.25	2883	4	2748	18
high common Pb (>1%)														
n5691-14c	47	28	42.1	0.53	1.04	-5.8	1.5925	1.02	0.267817	0.44	3293	7	3141	25
n5691-02c	45	27	34.5	0.51	1.54	-17.9	1.8676	1.04	0.258281	0.67	3236	11	2764	23
n5691-12c	37	38	26.9	1.06	7.13	-7.5	2.0596	1.03	0.187479	1.47	2720	24	2551	22
n5691-08c	1048	458	494.2	0.35	1.92	-15.3	2.6846	0.86	0.150279	0.87	2349	15	2041	15

[1]n5691 is the NordSIMS laboratory number for sample identification.

[2]Percentage of common ^{206}Pb in measured ^{206}Pb, calculated from the ^{204}Pb signal assuming a present-day Stacey & Kramers (1975) model terrestial Pb-isotope composition.

[3]Values corrected for common Pb.

Table 4. SIMS U-Th-Pb data for sample L1411, n5695 from St John's Harbour

Sample[1] spot #	U ppm	Th ppm	Pb ppm	Th/U	$f^{206}Pb$[2] %	Disc. %	Ratios[3] $^{238}U/^{206}Pb$	±σ (%)	$^{207}Pb/^{206}Pb$	±σ (%)	Ages[3] $^{207}Pb/^{206}Pb$	±σ	$^{206}Pb/^{238}U$	±σ
n5695-21c	50	15	57.4	0.24	0.42	-0.7	1.2594	1.35	0.369323	0.74	3789	11	3768	39
n5695-28c	148	44	161.6	0.27	0.12	-3.5	1.3115	1.50	0.360786	0.62	3753	9	3653	42
n5695-12c	180	101	212.3	0.54	0.37	-0.5	1.2737	1.11	0.360297	0.26	3751	4	3735	32
n5695-17c	164	55	175.7	0.27	0.32	-5.0	1.3358	1.25	0.359181	0.40	3746	6	3602	34
n5695-4c	569	437	696.4	0.75	0.10	1.0	1.2641	1.05	0.354920	0.22	3728	3	3757	30
n5695-7c	299	178	339.1	0.52	0.32	-2.0	1.3121	1.05	0.350588	0.20	3710	3	3652	29
n5695-13c	998	329	1079.4	0.30	0.26	-1.6	1.3167	1.13	0.345822	0.53	3689	8	3642	32
n5695-3c	249	122	275.4	0.46	0.10	-1.9	1.3252	1.16	0.343184	0.93	3677	14	3624	32
n5695-14c	234	159	246.1	0.40	0.45	-5.0	1.3760	1.08	0.339806	0.24	3662	4	3521	29
n5695-31c	397	111	429.0	0.26	0.10	0.5	1.3010	1.05	0.339603	0.31	3661	5	3676	30
n5695-25r	1076	468	1152.3	0.35	0.60	-2.0	1.3375	1.00	0.338496	0.11	3656	2	3599	28
n5695-6c	754	293	792.7	0.32	0.23	-2.9	1.3530	1.06	0.336788	0.23	3648	3	3567	29
n5695-5r	290	61	298.6	0.16	0.14	-1.4	1.3370	1.08	0.335013	0.28	3640	4	3600	30
n5695-30c	354	160	365.8	0.35	0.73	-4.2	1.3813	1.09	0.332274	0.31	3628	5	3511	30
n5695-5c	292	86	304.4	0.27	0.09	-0.7	1.3438	1.08	0.327402	0.26	3605	4	3586	30
n5695-24c	736	192	744.0	0.19	0.36	-2.0	1.3625	1.02	0.326837	0.21	3602	3	3548	28
>5% disc.														
n5695-25c	375	181	382.4	0.30	0.86	-6.9	1.4001	1.04	0.341983	0.19	3672	3	3474	28
n5695-29c	146	25	138.7	0.09	0.39	-6.8	1.4295	1.21	0.328403	0.42	3610	6	3419	32
n5695-26c	638	156	605.1	0.15	0.42	-6.0	1.4375	1.08	0.320394	0.30	3572	5	3404	29
n5695-9r	1163	386	1057.4	0.25	0.66	-9.0	1.5173	1.00	0.308317	0.12	3513	2	3264	26
n5695-20r	2805	118	730.1	0.01	0.97	-28.5	4.2830	1.02	0.111410	0.40	1823	7	1353	12
high common Pb (>1%)														
n5695-9c	314	169	303.9	0.31	1.45	-13.2	1.4872	1.05	0.347611	0.25	3697	4	3315	27
n5695-22c	156	127	136.9	0.14	2.53	-18.1	1.5801	1.16	0.346240	0.49	3691	7	3161	29
n5695-18c	88	53	80.9	0.14	6.00	-14.1	1.5106	1.36	0.344910	0.73	3685	11	3275	35
n5695-15c	141	65	134.0	0.28	1.05	-12.6	1.4985	1.25	0.338494	0.36	3656	5	3296	32
n5695-19c1	158	80	146.6	0.19	1.79	-11.4	1.4932	1.12	0.332296	0.45	3628	7	3305	29

n5695-19c2	413	134	418.3	0.26	1.35	-4.0	1.3823	1.06	0.331061	0.27	3622	4	3509	29
n5695-1c	287	107	272.9	0.21	1.10	-8.3	1.4602	1.07	0.325739	0.24	3597	4	3363	28
n5695-27c	660	259	518.7	0.07	1.78	-17.9	1.6896	1.21	0.306035	0.27	3501	4	2997	29
n5695-10c	414	78	346.0	0.08	1.08	-12.2	1.5871	1.06	0.303143	0.33	3486	5	3150	26
n5695-16c	435	141	354.9	0.10	3.13	-12.9	1.6248	1.04	0.295130	0.55	3445	9	3092	26
n5695-8c	540	173	387.7	0.09	1.26	-21.6	1.8353	1.09	0.287292	0.35	3403	5	2804	25
n5695-20c	354	367	184.7	0.04	5.85	-36.2	2.4375	1.20	0.252296	0.50	3199	8	2216	23
n5695-23c	979	253	664.4	0.10	1.31	-14.0	1.8711	1.02	0.239411	0.60	3116	10	2760	23
n5695-2c	1645	174	863.7	0.04	1.56	-22.9	2.3223	1.06	0.204289	0.57	2861	9	2308	21
n5695-11c	2741	996	1290.0	0.23	1.94	-32.2	2.7332	1.00	0.194611	0.23	2782	4	2010	17

[1]n5695 is the NordSIMS laboratory number for sample identification.
[2]Percentage of common 206Pb in measured 206Pb, calculated from the 204Pb signal assuming a present-day Stacey & Kramers (1975) model terrestial Pb-isotope composition.
[3]Values corrected for common Pb.

Table 5. SIMS U-Th-Pb data for sample L1443, n5536 from Big Island

Sample[1]	U	Th	Pb	Th/U	$f^{206}Pb$[2]	Disc. %	Ratios[3]				Ages[3]			
spot #	ppm	ppm	ppm		%		$^{238}U/^{206}Pb$	±σ (%)	$^{207}Pb/^{206}Pb$	±σ (%)	$^{207}Pb/^{206}Pb$	±σ	$^{206}Pb/^{238}U$	±σ
n5536-06c2	149	64	176.1	0.45	0.03	1.0	1.2510	1.63	0.362237	0.76	3759	11	3787	47
n5536-9c	421	290	508.1	0.67	0.41	-0.6	1.2740	1.40	0.360534	0.33	3752	5	3735	40
n5536-03r2	179	42	199.1	0.25	0.02	-1.0	1.2799	1.26	0.360166	0.27	3751	4	3722	36
n5536-07r	363	30	396.2	0.09	0.01	0.2	1.2669	1.30	0.359058	0.27	3746	4	3751	37
n5536-03c	266	148	320.9	0.57	0.01	1.7	1.2485	1.51	0.358953	0.25	3745	4	3793	44
n5536-14c	421	96	458.2	0.23	0.51	-2.4	1.3025	0.88	0.357765	0.21	3740	3	3672	25
n5536-07c	310	208	361.3	0.67	0.15	-3.1	1.3160	1.57	0.356160	0.27	3734	4	3644	44
n5536-14r	127	37	138.8	0.29	{0.01}	-2.5	1.3081	0.93	0.355755	0.26	3732	4	3661	26
n5536-12c2	153	92	178.6	0.61	0.22	-1.7	1.2973	1.53	0.355614	0.24	3731	4	3684	43
n5536-10c	218	83	240.2	0.36	0.68	-3.3	1.3203	0.89	0.355352	0.19	3730	3	3635	25
>5% disc.														
n5536-19c	329	201	371.6	0.59	0.53	-5.6	1.3469	1.57	0.358136	0.42	3742	6	3580	43
n5536-02c	250	109	271.8	0.41	0.70	-6.0	1.3535	1.94	0.357122	0.21	3738	3	3566	53

n5536-1c	261	201	262.3	0.47	0.92	-13.3	1.4844	1.31	0.349673	0.32	3706	5	3320	34
n5536-02r1	276	43	270.7	0.12	0.15	-8.7	1.4122	2.12	0.348604	0.25	3701	4	3451	57
n5536-17c	349	175	372.8	0.50	0.82	-5.9	1.3861	0.99	0.341106	0.36	3668	5	3501	27
n5536-04c	211	80	207.0	0.31	0.70	-10.3	1.4575	1.39	0.340138	0.32	3663	5	3368	36
n5536-10r2	131	30	118.6	0.20	0.37	-14.0	1.5394	0.93	0.332292	0.28	3628	4	3227	24
n5536-9r	128	31	122.6	0.24	0.08	-6.6	1.4440	0.93	0.321078	0.33	3575	5	3392	25
n5536-19r	550	56	381.7	0.09	0.25	-24.5	1.9027	0.98	0.287621	0.37	3405	6	2723	22
n5536-11c1	672	567	462.4	0.53	0.24	-24.1	2.0815	3.93	0.246153	4.69	3160	72	2529	83
high common Pb (>1%)														
n5536-12c1	111	33	121.5	0.29	3.35	-3.3	1.3126	1.43	0.359213	0.45	3747	7	3651	40
n5536-06c1	386	246	437.4	0.58	5.18	-4.7	1.3354	1.67	0.357345	1.01	3739	15	3603	46
n5536-05c	348	216	394.1	0.57	6.28	-4.0	1.3304	1.79	0.354526	1.45	3727	22	3614	50
n5536-16c1	307	99	337.2	0.29	2.16	-1.9	1.3025	0.89	0.354406	0.17	3726	3	3673	25
n5536-05r1	290	56	302.2	0.18	1.59	-4.7	1.3441	1.49	0.353034	0.26	3720	4	3585	41
n5536-16c2	359	202	409.9	0.53	3.10	-2.0	1.3072	1.16	0.352947	0.57	3720	9	3663	32
n5536-13r	294	154	331.4	0.51	1.08	-2.6	1.3177	0.92	0.351742	0.30	3715	5	3640	26
n5536-10r1	276	41	294.2	0.14	1.83	-1.4	1.3022	0.91	0.351516	0.23	3714	4	3673	25
n5536-06r	439	104	409.0	0.21	4.10	-15.2	1.5172	1.58	0.349913	0.33	3707	5	3264	41
n5536-20r	252	42	269.0	0.15	1.18	-1.0	1.3009	1.31	0.349362	0.29	3704	4	3676	37
n5536-18c	352	41	357.7	0.10	2.16	-5.0	1.3553	1.03	0.349271	0.34	3704	5	3563	28
n5536-08c	552	721	647.6	1.17	1.35	-8.6	1.4282	1.86	0.340998	1.94	3667	29	3421	50
n5536-20c	402	265	396.7	0.59	3.16	-13.8	1.5336	1.22	0.333295	0.38	3632	6	3236	31
n5536-01r	604	514	618.7	0.66	2.76	-11.1	1.4886	1.43	0.332760	0.31	3630	5	3313	37
n5536-05r2	179	71	169.3	0.30	4.36	-11.3	1.4978	1.44	0.330053	0.41	3617	6	3297	37
n5536-13c	352	198	373.5	0.53	1.32	-4.3	1.3905	1.53	0.328930	0.46	3612	7	3493	42
n5536-11c2	543	405	412.1	0.49	5.68	-21.8	1.8954	2.51	0.272854	3.55	3323	54	2731	56
a mixture of growth zones														
n5536-08r1	165	40	180.7	0.24	0.06	-0.3	1.2907	1.45	0.349607	0.29	3705	4	3698	41
n5536-15c	186	42	199.8	0.22	0.15	-1.5	1.3074	0.90	0.349505	0.22	3705	3	3662	25
n5536-02r2	117	39	129.4	0.33	0.21	0.3	1.2909	1.33	0.345856	0.47	3689	7	3698	38
n5536-08r2	351	41	367.4	0.12	0.02	-0.5	1.3099	1.48	0.341741	0.42	3671	6	3657	41

n5536-03r1	136	40	131.1	0.29	{0.01}	-3.7	1.4372	1.30	0.307162	0.90	3507	14	3405	34

[1]n5536 is the NordSIMS laboratory number for sample identification.
[2]Percentage of common 206Pb in measured 206Pb, calculated from the 204Pb signal assuming a present-day Stacey & Kramers (1975) model terrestial Pb-isotope composition.
[3]Values corrected for common Pb.

Table 6. SIMS U-Th-Pb data for sample L1444, n5535 from Big Island

Sample[1]	U	Th	Pb	Th/U	$f^{206}Pb$[2]	Disc. %	Ratios[3]				Ages[3]			
spot #	ppm	ppm	ppm		%		$^{238}U/^{206}Pb$	±σ (%)	$^{207}Pb/^{206}Pb$	±σ (%)	$^{207}Pb/^{206}Pb$	±σ	$^{206}Pb/^{238}U$	±σ
n5535-07r	214	107	186.5	0.42	0.21	-1.9	1.5711	1.29	0.256413	0.44	3225	7	3175	32
n5535-02r	508	236	453.1	0.42	0.40	0.5	1.5326	1.25	0.256341	0.25	3224	4	3238	32
n5535-01c	78	30	66.7	0.32	0.53	-1.2	1.5619	1.79	0.255653	0.93	3220	15	3190	45
n5535-04c	312	188	287.0	0.54	0.66	1.8	1.5174	1.73	0.255131	0.82	3217	13	3263	45
n5535-06r1	368	149	325.1	0.36	0.09	1.2	1.5283	1.22	0.254797	0.28	3215	4	3245	31
n5535-02c	205	113	182.1	0.46	0.14	-0.4	1.5537	1.42	0.254381	0.82	3212	13	3203	36
n5535-01r	223	112	195.5	0.43	0.44	-0.4	1.5594	1.39	0.252930	0.47	3203	7	3194	35
high common Pb (>1%)														
n5535-07c1	122	35	99.1	0.22	2.13	-4.8	1.6233	1.60	0.255015	0.60	3216	9	3094	39
n5535-06c2	114	50	95.5	0.34	3.59	-3.7	1.6061	1.74	0.254671	1.35	3214	21	3120	43
n5535-09r	221	104	182.3	0.35	3.03	-5.5	1.6413	1.24	0.253827	0.46	3209	7	3067	30
n5535-10r	158	63	114.2	0.26	12.38	-15.8	1.8465	1.44	0.252734	0.97	3202	15	2790	33
n5535-03c	286	239	263.1	0.72	1.71	-1.1	1.5729	1.31	0.252575	0.68	3201	11	3172	33
n5535-09c	387	347	306.3	0.44	10.91	-10.5	1.7451	1.45	0.250760	3.56	3190	55	2920	34
n5535-05c	351	168	268.8	0.33	5.90	-10.8	1.7593	1.26	0.248859	1.30	3178	20	2901	30
n5535-07c2	135	61	105.8	0.34	2.32	-6.4	1.7076	1.66	0.241866	0.83	3132	13	2972	40
n5535-05r	203	19	[133]	no data	9.96	-22.9	2.1679	1.37	0.226043	1.79	3024	28	2445	28
n5535-08c	1196	328	603.7	0.14	24.88	-29.0	2.4962	1.70	0.207198	1.85	2884	30	2172	31
a mixture of growth zones														
n5535-10c	1242	631	1076.5	0.47	0.51	-0.9	1.5865	1.16	0.248349	0.14	3174	2	3151	29
n5535-06c	95	39	79.6	0.34	0.24	-1.0	1.5975	1.84	0.246057	0.57	3160	9	3134	46

[1]n5535 is the NordSIMS laboratory number for sample identification.

[2]Percentage of common 206Pb in measured 206Pb, calculated from the 204Pb signal assuming a present-day Stacey & Kramers (1975) model terrestial Pb-isotope composition.
[3]Values corrected for common Pb.

Table 7. SIMS U-Th-Pb data for sample L1463, n5538 from Little Island

Sample[1]	U	Th	Pb	Th/U	$f^{206}Pb$[2]	Disc. %	Ratios[3]				Ages[3]			
spot #	ppm	ppm	ppm		%		$^{238}U/^{206}Pb$	±σ (%)	$^{207}Pb/^{206}Pb$	±σ (%)	$^{207}Pb/^{206}Pb$	±σ	$^{206}Pb/^{238}U$	±σ
n5538-11c1	42	19	49.9	0.46	{0.06}	0.9	1.2558	1.08	0.359852	0.49	3749	7	3776	31
n5538-01c	398	70	421.1	0.16	0.11	-3.1	1.3195	1.39	0.354243	0.32	3725	5	3636	39
n5538-12c	379	238	440.5	0.60	0.48	-1.7	1.3013	1.03	0.354093	0.29	3725	4	3675	29
n5538-04r1	360	108	402.5	0.31	0.16	-0.1	1.2823	1.25	0.352753	0.23	3719	4	3717	35
n5538-10c	500	166	565.3	0.33	0.03	0.9	1.2712	0.89	0.351886	0.13	3715	2	3741	25
n5538-20c	444	173	505.5	0.39	0.06	0.7	1.2754	0.78	0.351430	0.16	3713	2	3732	22
n5538-03c1	284	57	309.0	0.20	0.05	0.1	1.2867	1.35	0.349162	0.33	3703	5	3707	38
n5538-19r	269	46	279.3	0.16	0.04	-3.6	1.3402	0.78	0.347496	0.20	3696	3	3593	22
n5538-08c1	207	60	222.5	0.26	0.23	-1.7	1.3168	1.46	0.346423	0.24	3691	4	3642	41
n5538-11c2	22	4	22.6	0.17	{0.10}	-1.8	1.3248	1.28	0.342825	0.59	3675	9	3625	36
n5538-08r2	1000	37	1012.4	0.04	0.03	-0.5	1.3274	1.45	0.333676	0.16	3634	3	3620	40
n5538-05r	936	44	943.0	0.05	0.08	1.2	1.3257	1.21	0.324562	0.45	3592	7	3623	34
n5538-02r1	1046	309	1018.1	0.27	0.05	-5.3	1.4314	1.61	0.318456	0.97	3562	15	3415	43
n5538-03c2	421	75	416.4	0.17	0.07	0.6	1.3695	2.03	0.309211	0.38	3517	6	3534	55
>5% disc.														
n5538-08r1	363	145	369.1	0.25	0.25	-7.7	1.3978	1.42	0.348500	0.17	3700	3	3479	38
n5538-02c2	308	74	310.5	0.22	0.44	-7.6	1.3958	1.45	0.348280	0.24	3699	4	3483	39
n5538-9c	581	123	557.1	0.18	0.37	-10.1	1.4521	0.89	0.340668	0.11	3666	2	3378	23
n5538-02c1	399	106	355.4	0.22	0.45	-16.2	1.5726	1.48	0.335250	0.56	3641	9	3173	37
n5538-22c	397	119	385.1	0.21	0.56	-7.0	1.4320	0.79	0.328768	0.14	3611	2	3414	21
n5538-17c	328	46	302.9	0.12	0.12	-9.2	1.4717	0.80	0.326598	0.18	3601	3	3342	21
n5538-13c	1012	31	884.2	0.03	0.05	-7.5	1.5018	0.77	0.304925	0.22	3495	3	3290	20
n5538-07r2	857	136	709.5	0.14	0.30	-13.2	1.6191	1.16	0.298957	0.28	3465	4	3100	29
n5538-01r	564	89	493.8	0.13	0.35	-6.2	1.5176	2.19	0.292487	1.50	3431	23	3263	56

n5538-07r1	1249	54	973.9	0.04	0.06	-12.6	1.6599	2.14	0.283284	0.72	3381	11	3040	52
n5538-14c	1014	17	765.4	0.03	0.09	-9.4	1.6825	1.50	0.260867	1.21	3252	19	3007	36
n5538-18c	1114	77	830.7	0.06	0.03	-6.3	1.6938	0.79	0.244463	0.30	3149	5	2991	19
n5538-02r2	3442	970	1300.0	0.16	0.44	-36.4	3.2791	2.12	0.166695	1.94	2525	32	1716	32
high common Pb (>1%)														
n5538-19c	17	7	18.2	0.44	2.69	-9.2	1.3899	2.16	0.362677	1.78	3761	27	3494	59
n5538-23c	150	44	142.1	0.21	1.87	-13.1	1.4891	0.86	0.346428	0.27	3691	4	3312	22
n5538-05c	487	138	516.8	0.33	2.12	-3.9	1.3510	1.53	0.344525	0.45	3683	7	3571	42
n5538-07c	274	139	261.1	0.27	1.02	-12.1	1.4895	1.35	0.339205	0.23	3659	3	3311	35
n5538-21c	212	57	131.4	0.23	4.91	-35.5	2.2264	1.10	0.287670	0.40	3405	6	2392	22
n5538-10r	2274	633	1443.4	0.18	1.50	-24.6	2.0706	0.86	0.251022	0.53	3191	8	2540	18
a mixture of growth zones														
n5538-16c	143	63	157.3	0.43	0.55	-2.5	1.3282	0.83	0.345926	0.29	3689	4	3618	23
n5538-15c	134	31	135.7	0.20	0.18	-3.5	1.3661	0.86	0.334667	0.23	3639	3	3541	23
n5538-06c	432	60	399.6	0.13	0.03	-2.9	1.4452	1.52	0.299432	1.07	3467	16	3390	40
n5538-11r	1025	4	738.8	0.00	0.02	-1.0	1.6996	0.90	0.223584	0.14	3007	2	2983	22
n5538-06r	1401	39	915.2	0.02	0.49	-6.2	1.8625	1.40	0.211457	0.62	2917	10	2771	32

[1]n5538 is the NordSIMS laboratory number for sample identification.
[2]Percentage of common 206Pb in measured 206Pb, calculated from the 204Pb signal assuming a present-day Stacey & Kramers (1975) model terrestial Pb-isotope composition.
[3]Values corrected for common Pb.

Table 8. SIMS U-Th-Pb data for sample L1467, n5694 from Maidmonts Island

Sample[1]	U	Th	Pb	Th/U	$f^{206}Pb$[2]	Disc. %	Ratios[3]				Ages[3]			
spot #	ppm	ppm	ppm		%		$^{238}U/^{206}Pb$	±σ (%)	$^{207}Pb/^{206}Pb$	±σ (%)	$^{207}Pb/^{206}Pb$	±σ	$^{206}Pb/^{238}U$	±σ
n5694-4c	565	489	550.1	0.82	0.06	-3.9	1.5404	0.88	0.273877	0.15	3328	2	3225	22
n5694-8c	36	21	34.8	0.59	{0.07}	0.1	1.4787	1.18	0.273875	0.52	3328	8	3330	31
n5694-12c	248	240	253.6	0.95	0.16	-0.8	1.4916	0.90	0.273855	0.18	3328	3	3308	23
n5694-2c	198	177	198.7	0.87	0.03	-0.9	1.4959	0.96	0.273068	0.26	3324	4	3300	25
n5694-20c	381	230	362.3	0.57	0.05	-1.2	1.4997	0.96	0.273051	0.19	3324	3	3294	25

n5694-18c	471	313	454.0	0.64	0.03	-1.1	1.4989	0.91	0.273024	0.14	3323	2	3295	23
n5694-1c	120	86	115.8	0.68	0.05	-1.6	1.5079	1.05	0.272452	0.34	3320	5	3279	27
n5694-3c	202	167	193.5	0.78	0.32	-4.4	1.5529	0.91	0.272384	0.30	3320	5	3205	23
n5694-13c	40	26	37.2	0.62	{0.02}	-3.1	1.5344	1.12	0.271622	0.44	3315	7	3235	28
n5694-21c	117	95	115.3	0.77	0.05	-0.6	1.4976	1.04	0.271324	0.37	3314	6	3297	27
n5694-5c	1250	756	1195.3	0.60	0.02	-0.4	1.4954	0.88	0.270896	0.08	3311	1	3301	23
n5694-14c	30	17	27.3	0.54	0.13	-3.8	1.5528	1.22	0.269669	0.52	3304	8	3205	31
n5694-23c	35	20	31.7	0.56	0.13	-3.9	1.5583	1.75	0.268602	1.39	3298	22	3196	44
n5694-22c	58	38	53.8	0.60	0.13	-3.8	1.5574	1.05	0.268410	0.42	3297	7	3197	27
n5694-15c	270	240	264.2	0.86	0.06	-2.0	1.5334	0.93	0.266794	0.17	3287	3	3237	24
n5694-27c	72	44	66.4	0.58	{0.04}	-2.6	1.5522	1.07	0.264443	0.43	3273	7	3206	27
n5694-6c	47	34	43.5	0.71	{0.08}	-3.9	1.5826	1.13	0.261602	0.64	3256	10	3157	28
>5% disc.														
n5694-4r	74	43	66.9	0.56	0.07	-6.9	1.5832	1.08	0.275623	0.43	3338	7	3156	27
n5694-26c	241	214	225.7	0.81	0.16	-7.2	1.6015	1.32	0.272117	0.31	3318	5	3127	33
n5694-19c	43	41	39.7	0.77	0.24	-7.6	1.6145	1.18	0.270394	0.48	3308	7	3108	29
n5694-24c	86	54	76.6	0.56	0.18	-6.4	1.5999	0.98	0.268540	0.42	3298	7	3130	24
n5694-11c	58	46	53.7	0.76	0.82	-5.7	1.5987	1.18	0.265448	0.67	3279	11	3132	29
n5694-7c	190	136	171.9	0.67	0.07	-5.7	1.6054	1.06	0.263834	0.32	3270	5	3121	26
n5694-25c	1004	12	672.0	0.01	0.33	-5.8	1.8231	0.91	0.217032	0.20	2959	3	2819	21
high common Pb (>1%)														
n5694-17c	458	411	434.0	0.84	1.45	-6.8	1.5942	0.98	0.272250	0.27	3319	4	3139	24
n5694-9c	158	121	155.5	0.95	11.23	-4.4	1.5611	0.93	0.270027	0.68	3306	11	3191	23
n5694-10c	52	72	52.2	1.69	32.39	-14.8	1.7759	1.25	0.263758	1.70	3269	27	2879	29
n5694-16c	217	79	153.4	0.30	1.01	-13.2	1.8790	1.04	0.234397	0.36	3082	6	2751	23

[1]n5694 is the NordSIMS laboratory number for sample identification.
[2]Percentage of common 206Pb in measured 206Pb, calculated from the 204Pb signal assuming a present-day Stacey & Kramers (1975) model terrestial Pb-isotope composition.
[3]Values corrected for common Pb.